

- therapy for chronic hepatitis C: a multicenter, prospective, randomized, controlled trial in Japan. *J Gastroenterol* 39: 570–574.
7. Kawamura Y, Akuta N, Sezaki H, Hosaka T, Someya T, et al. (2005) Determinants of serum ALT normalization after phlebotomy in patients with chronic hepatitis C infection. *J Gastroenterol* 40: 901–906.
 8. Sumida Y, Kanemasa K, Fukumoto K, Yoshida N, Sakai K (2007) Effects of dietary iron reduction versus phlebotomy in patients with chronic hepatitis C: results from a randomized, controlled trial on 40 Japanese patients. *Intern Med* 46: 637–642.
 9. Yano M, Hayashi H, Wakusawa S, Sanae F, Takikawa T, et al. (2002) Long term effects of phlebotomy on biochemical and histological parameters of chronic hepatitis C. *Am J Gastroenterol* 97: 133–137.
 10. Kato J, Kobune M, Nakamura T, Kuroiwa G, Takada K, et al. (2001) Normalization of elevated hepatic 8-hydroxy-2-deoxyguanosine levels in chronic hepatitis C patients by phlebotomy and low iron diet. *Cancer Res* 61: 8697–8702.
 11. Brissot P, Degnignier Y. Haemochromatosis In: McIntyre N, Benhamou JP, Bircher J, Rizzetto M, Rodes J, eds. Oxford textbook of clinical hepatology Oxford: Oxford University Press. pp 1379–1391.
 12. Olthof AW, Sijens PE, Kreeftenberg HG, Kappert P, Irwan R, et al. (2007) Correlation between serum ferritin levels and liver iron concentration determined by MR imaging: impact of hematologic disease and inflammation. *Magn Reson Imaging* 25: 228–231.
 13. Alústiza JM, Castiella A, De Juan MD, Emparanza JI, Artetxe J, et al. (2007) Iron overload in the liver diagnostic and quantification. *Eur J Radiol* 61: 499–506.
 14. Alustiza JM, Artetxe J, Castiella A, Agirre C, Emparanza JI, et al. (2004) Gipuzkoa Hepatic Iron Concentration by MRI Study Group. MR quantification of hepatic iron concentration. *Radiology* 230: 479–484.
 15. Gandon Y, Olivieri D, Guyader D, Aubé C, Oberti F, et al. (2004) Non-invasive assessment of hepatic iron stores by MRI. *Lancet* 363: 357–362.
 16. St Pierre TG, Clark PR, Chua-anusorn W, Fleming AJ, Jeffrey GP, et al. (2005) Noninvasive measurement and imaging of liver iron concentrations using proton magnetic resonance. *Blood* 105: 855–861.
 17. Olthof AW, Sijens PE, Kreeftenberg HG, Kappert P, van der Jagt EJ, et al. (2009) Non-invasive liver iron concentration measurement by MRI: Comparison of two validated protocols. *Eur J Radiol* 71: 116–121.
 18. Bonkovsky HL, Rubin RB, Cable EE, Davidoff A, Rijcken TH, et al. (1999) Hepatic iron concentration: noninvasive estimation by means of MR imaging techniques. *Radiology* 212: 227–234.
 19. Gandon Y, Guyader D, Heautot JF, Reda MI, Yaouanq J, et al. (1994) Hemochromatosis: diagnosis and quantification of liver iron with gradient-echo MR imaging. *Radiology* 193: 533–538.
 20. Kreeftenberg HG, Jr., Mooyaart EL, Huizenga JR, Sluiter WJ (2000) Quantification of liver iron concentration with magnetic resonance imaging by combining T1-, T2-weighted spin echo sequences and a gradient echo sequence. *Neth J Med* 56: 133–137.
 21. Bammer R, Keeling SL, Augustin M, Pruessmann KP, Wolf R, et al. (2001) Improved diffusion weighted single-shot echo-planar imaging (EPI) in stroke using sensitivity encoding (SENSE). *Magn Reson Med* 46: 548–554.
 22. Taouli B, Martin AJ, Qayyum A, Merriman RB, Vigneron D, et al. (2004) Parallel imaging and diffusion tensor imaging for diffusion weighted MRI of the liver: preliminary experience in healthy volunteers. *AJR Am J Roentgenol* 183: 677–680.
 23. Murtz P, Flacke S, Traber F, van den Brink JS, Gieseke J, et al. (2002) Abdomen: diffusion-weighted MR imaging with pulse-triggered single-shot sequences. *Radiology* 224: 258–264.
 24. Tanimoto A, Kuribayashi S (2006) Application of superparamagnetic iron oxide to imaging of hepatocellular carcinoma. *Eur J Radiol* 58: 200–216.
 25. Coenegrachts K, Matos C, Ter Beek L, Metens T, Haspelslagh M, et al. (2009) Focal liver lesion detection and characterization: Comparison of non-contrast enhanced and SPIO-enhanced diffusion-weighted single-shot spin echo echo planar and turbo spin echo T2-weighted imaging. *Eur J Radiol* 72: 432–439.
 26. Griesmann GE, Hartmann AC, Farris FF (2009) Concentrations and correlations for eight metals in human liver. *Int J Environ Health Res* 19: 231–238.
 27. Ishak K, Baptista A, Bianchi L, Callea F, De Groote J, et al. (1995) Histological grading and staging of chronic hepatitis. *J Hepatol* 22: 696–699.
 28. Kleiner DE, Brunt EM, Van Natta M, Behling C, Contos MJ, et al. (2005) ; Nonalcoholic Steatohepatitis Clinical Research Network. Design and validation of a histological scoring system for nonalcoholic fatty liver disease. *Hepatology* 41: 1313–1321.
 29. Brunt EM, Janney CG, Di Bisceglie AM, Neuschwander-Tetri BA, Bacon BR (1999) Nonalcoholic steatohepatitis: a proposal for grading and staging the histological lesions. *Am J Gastroenterol* 94: 2467–2474.
 30. Fujimoto K, Tonan T, Azuma S, Kage M, Nakashima O, et al. (2011) Evaluation of the mean and entropy of apparent diffusion coefficient values in chronic hepatitis C: Correlation with pathologic fibrosis stage and inflammatory activity grade. *Radiology* 258: 739–748.
 31. Tonan T, Fujimoto K, Qayyum A, Azuma S, Ishibashi M, et al. (2011) Correlation of Kupffer cell function and hepatocyte function in chronic viral hepatitis evaluated with superparamagnetic iron oxide-enhanced magnetic resonance imaging and scintigraphy using technetium-99m-labelled galactosyl human serum albumin. *Exp Ther Med* 2: 607–613.
 32. Bland JM, Altman DG (1986) Statistical methods for assessing agreement between two methods of clinical measurement. *Lancet* 1: 307–310.
 33. Akaike H (1974) A new look at the statistical model identification. *IEEE Trans Automatic Control* 19: 716–723.
 34. Stone M (1974) Cross-validatory choice and assessment of statistical predictions. *Journal of Royal Statistical Society B* 36: 111–147.
 35. Kawaguchi A, Yonemoto K, Tanizaki Y, Kiyohara Y, Yanagawa T, et al. (2008) Application of functional ANOVA models for hazard regression to the Hisayama data. *Stat Med* 27: 3515–3527.
 36. Lim RP, Tuvia K, Hajdu CH, Losada M, Gupta R, et al. (2010) Quantification of hepatic iron deposition in patients with liver disease: comparison of chemical shift imaging with single-echo T2*-weighted imaging. *AJR Am J Roentgenol* 194: 1288–1295.
 37. Taouli B, Sandberg A, Stemmer A, Parikh T, Wong S, et al. (2009) Diffusion-weighted imaging of the liver: comparison of navigator triggered and breathhold acquisitions. *J Magn Reson Imaging* 30: 561–568.
 38. Nasu K, Kuroki Y, Sekiguchi R, Nawano S (2006) The effect of simultaneous use of respiratory triggering in diffusion weighted imaging of the liver. *Magn Reson Med Sci* 5: 129–136.
 39. Gourtsoyianni S, Papanikolaou N, Yarmenitis S, Maris T, Karantanis A, et al. (2008) Respiratory gated diffusion weighted imaging of the liver: value of apparent diffusion coefficient measurements in the differentiation between most commonly encountered benign and malignant focal liver lesions. *Eur Radiol* 18: 486–492.
 40. Asbach P, Klessen C, Kroencke TJ, Kluner C, Stemmer A, et al. (2005) Magnetic resonance cholangiopancreatography using a free-breathing T2-weighted turbo spin echo sequence with navigator-triggered prospective acquisition correction. *Magn Reson Imaging* 23: 939–945.
 41. Westphalen AC, Qayyum A, Yeh BM, Merriman RB, Lee JA, et al. (2007) Liver fat: effect of hepatic iron deposition on evaluation with opposed-phase MR imaging. *Radiology* 242: 450–455.
 42. Taouli B, Tolia AJ, Losada M, Babb JS, Chan ES, et al. (2007) Diffusion-weighted MRI for quantification of liver fibrosis: preliminary experience. *AJR Am J Roentgenol* 189(4): 799–806.
 43. Taouli B, Chouli M, Martin AJ, Qayyum A, Coakley FV, et al. (2008) Chronic hepatitis: role of diffusion-weighted imaging and diffusion tensor imaging for the diagnosis of liver fibrosis and inflammation. *J Magn Reson Imaging* 28(1): 89–95.

Clinical Relevance and Sequence Analysis of the *Helicobacter pylori dupA* Region from Two Areas in Japan with Different Gastric Cancer Risks

Hidetaka Matsuda¹, Yoshiyuki Ito¹, Hiroyuki Suto¹, Akiyo Yamakawa¹, Satoko Satomi¹, Masahiro Ohtani^{1,2}, Yukinao Yamazaki^{1,2}, Yukinori Kusaka³, Yoshiki Shimabukuro⁴, Kaoru Kikuchi⁴, Yoshihide Keida⁴, Takeshi Azuma⁵, Yasunari Nakamoto¹

¹Second Department of Internal Medicine, Faculty of Medical Sciences, University of Fukui, Fukui 910-1193, Japan; ²Department of Endoscopic Medicine, University of Fukui Hospital, University of Fukui, Fukui 910-1193, Japan; ³Department of Environmental Health, Faculty of Medical Sciences, University of Fukui, Fukui 910-1193, Japan; ⁴Division of Internal Medicine, Okinawa Chubu Hospital, Okinawa 904-2293, Japan; ⁵Frontier Medical Science in Gastroenterology, International Center for Medical Research and Treatment, Kobe University School of Medicine, Kobe 650-0017, Japan

Abstract

Background & Aims: We investigated the virulence and sequences of duodenal ulcer-promoting gene A (*dupA*) of *Helicobacter pylori* (*H. pylori*) isolated from 2 areas in Japan with different gastric cancer risks.

Methods: The *dupA* status of 248 Japanese *H. pylori* strains (111 from Fukui and 137 from Okinawa) isolated from patients with duodenal ulcers, gastric ulcers, chronic gastritis, or gastric cancer was evaluated by dot-blot hybridization followed by polymerase chain reaction. Sequence analyses of *dupA* and its upstream region were performed in 15 strains.

Results: In both areas, no significant association was observed between *dupA* and the evaluated clinical outcomes. In a multivariable logistic regression, *dupA* positivity was independently associated with strains isolated from Okinawa, showing the lowest incidence of gastric cancer in Japan, and with East Asian-type *cagA* positivity (odds ratio [OR]=2.128, 95% confidence interval [CI] =1.146–3.949 and OR=12.924, 95% CI=1.689–98.901, respectively). Sequence alignment showed *dupA* was divided into 2 genotypes: a Shi470-type (2499 bp) and a J99-type (1839 bp). Among 60 *dupA*⁺ Japanese strains, 58 (96.7%) were of the Shi470-type and 2 of the J99-type. The nucleotide sequences of 13 Shi470-type Japanese isolates from both areas were highly homologous (98.9%) to each other and a remote Amazonian strain, Shi470. Of these, 12 (92.3%) carried intact full-length *dupA*.

Conclusion: In Japan, *dupA* appeared to be associated with East Asian-type *cagA* and with host residence in Okinawa. The intact genotype of the Shi470-type *dupA* was the major form in Japan.

Immunogastroenterology 2012; 1:127-135

Key words

Helicobacter pylori; *dupA*; *cagA*; virulence factors; type IV secretion system; Okinawa

Introduction

Chronic *Helicobacter pylori* (*H. pylori*) infection is a definitive risk factor for various gastroduodenal diseases such as peptic ulcers, gastric adenocarcinoma, and gastric mucosa-associated lymphoid tissue lymphoma.¹⁻³ Although the mechanism of this infection in humans has been extensively studied, no definitive explanation has been obtained. Although infection with strains producing cytotoxin-associated gene A antigen (*CagA*) and vacuolating cytotoxin (*VacA*) are reported to increase the risk of severe gastroduodenal diseases in the West, this association has not been demonstrated in East Asia.⁴⁻¹⁰ In addition, none of the reported virulence factors including *cagA* and *vacA* expression has

been confirmed to be a definitive marker for any single specific clinical outcome.¹¹⁻¹³

H. pylori exhibits a higher degree of genomic and allelic diversity than most other bacterial species, and significant geographic differences exist among strains.¹⁴⁻¹⁶ Geographic diversity in the *H. pylori* virulence genes has been associated with different regional prevalences in gastroduodenal diseases; the prevalence of gastric cancer (GC) is higher in Japan than in other countries.^{17,18} However, Okinawa has the lowest prevalence of GC in Japan and approximately half of that in other prefectures.¹⁹ On the other hand, the prevalence of *H. pylori* in Okinawa does not differ significantly from those in other parts of Japan.²⁰ To investigate the differences in the prevalence of GC between Okinawa and other prefectures in Japan, we previously analyzed the sequences of *H. pylori* virulence genes isolated from patients in 2 distinct Japanese areas (Okinawa and Fukui) and found that the genotypes of *cagA* were the most important factor causing the discrepancy.^{19,21-27}

Recently, Lu et al. described a novel *H. pylori* virulence factor,

Yasunari Nakamoto, Second Department of Internal Medicine, Faculty of Medical Sciences, University of Fukui, Fukui 910-1193, Japan; Email: nakamoto-med2@med.u-fukui.ac.jp

Submitted: 26/02/2012; Revised: 20/03/2012; Accepted: 12/06/2012

DOI: 10.7178/ig.21

designated duodenal ulcer-promoting gene A (*dupA*).²⁸ *dupA* comprises 2 genes—*jhp0917* and *jhp0918*—present in the *H. pylori* plasticity zone. A single base-pair insertion (C or T) in the 3' region of *jhp0917* confers a continuous 1839 bp open reading frame (ORF). As *dupA* shows homology to *virB4*, a *virB/D* homolog gene encoding the type IV secretion system (T4SS) of *Agrobacterium tumefaciens*, this gene is considered a component of a novel TFSS of *H. pylori*.^{11,28-30}

Infection with *dupA*⁺ strains is associated with increased interleukin-8 (IL-8) production from the gastric antral mucosa and the development of duodenal ulcers (DUs), in 3 different countries (Japan, Korea, and Colombia). Infection with the *dupA*⁺ strain is also a potential protective factor against atrophic gastritis and GC.²⁸ However, subsequent studies in various geographic areas were unable to confirm the close association between *dupA* and clinical outcomes.³¹⁻⁴² Moreover, the findings of previous Japanese studies have been inconsistent.^{28,39,40}

The association between the presence of *dupA* and other virulent factors of *H. pylori* remains largely unexamined. Although some previous studies have discussed the association between the statuses of *dupA* and *cagA*,^{31-35,37,42} the genetic diversity of *cagA* (i.e., the East Asian-type or the Western-type) was not considered. Similarly, the genetic structure of *dupA* is not well known. Most previous studies analyzed the limited nucleotide sequences corresponding to *jhp0917* and *jhp0918*,^{28,31,33,34,36,38,39,41,43,44} but only a few have investigated the surrounding *dupA* regions, especially the upstream ones, which may regulate *dupA* expression.^{30,45,46} In this study, we aimed to examine whether (i) *dupA* could be a disease-specific risk determinant in Japan; (ii) *dupA* could explain the lower risk of GC in Okinawa; and (iii) *dupA* and *cagA* statuses were associated, even when the genotypes of *cagA* (i.e., the East Asian or Western genotype) were considered. We also discuss whether the genetic diversity of the *dupA* upstream region exists among the groups of clinical isolates in Japan.

Materials and Methods

H. pylori strains, culture, and DNA extraction

A total of 248 clinical *H. pylori* isolates were obtained from Japanese patients (111 patients in Fukui and 137 in Okinawa) during upper gastrointestinal endoscopy performed at the University of Fukui Hospital, Fukui, and Okinawa Chubu Hospital, Okinawa. The patient group in Fukui comprised 20 patients with DU, 20 with gastric ulcer (GU), 39 with chronic gastritis, and 32 with GC. The patient group in Okinawa comprised 26 patients with DU, 18 with GU, 60 with chronic gastritis, and 33 with GC. This study was performed according to the principles of the Declaration of Helsinki. Informed consent was obtained from each patient and the institutional ethics committee approved the study protocol. The presence of *H. pylori* in a patient was confirmed through positive results of the rapid urease test (RUT), the C13 urea breath test (UBT), or a histological analysis. The clinical diagnosis was established by endoscopic findings. In addition, the diagnosis of GC was histologically confirmed in all cases. *H. pylori* culture and DNA extractions were conducted as described previously.²¹⁻²⁵ Patients

from whom *H. pylori* could not be cultured were excluded from the study.

H. pylori sequence analysis

The primers used in this study are shown in **table 1** and **figure 1**. The presence of *dupA* was defined by both dot-blot hybridization and polymerase chain reaction (PCR) as described below.

Dot-blot hybridization was performed using Hybond-N⁺ nylon membranes (GE Healthcare Lifesciences, Uppsala, Sweden) containing 10–20 ng aliquots of genomic DNA per spot from each strain of interest and hybridization probes labeled using the enhanced chemiluminescence kit (AmershamTM ECLTM Direct Nucleic Acid Labeling and Detection System; GE Healthcare Lifesciences), according to the manufacturer's instructions. Probes for the 2 *dupA* segments (*jhp0917* and *jhp0918*) were generated by PCR from J99 genomic DNA with primers JHP0917(+) and JHP0917(-) (307 bp product) and JHP0918-1F and JHP0918-1R (377 bp product). The PCR-amplified DNAs were purified using the MinElute Gel Extraction Kit (Qiagen, Hilden, Germany) prior to ECL labeling for use in hybridization according to the manufacturer's instructions. A probe for *ureI* (a housekeeping gene of *H. pylori*) was used as a positive control for hybridization.

Following the dot-blot hybridization, PCR was performed using the DupAF113/R1083 and DupAFb/Rb primer pairs. Specific PCR and DNA sequencing was conducted as described previously.²¹⁻²⁷ The PCR products were purified on Centricon-100 Concentrator columns (Amicon, Beverly, MA, USA) and then sequenced directly using the BigDye Terminator Cycle Sequencing Ready Reaction Mix (Applied Biosystems, Foster City, CA, USA) in an ABI PRISM 310 Genetic Analyzer (Applied Biosystems). Cycle sequencing reactions were performed for both strands. DNA sequencing editing and analysis were performed with GENETYX-MAC software version 14.0.1 (GENETYX Corporation, Tokyo, Japan).

For the dot-blot hybridization, the tested strains were considered *dupA*⁺ or *dupA*⁻ if the *jhp0917* and *jhp0918* genes were both present or absent, respectively. When a strain was positive for only one of these genes, the *dupA* status was defined in accordance with the PCR results. For the PCR assay, only strains showing both DupAF113/R1083 and DupAFb/Rb positivity were considered *dupA*⁺, while all the remaining strains were defined as *dupA*⁻. Both assays were performed for all strains. If a strain showed discrepant results between the 2 tests, the PCR result was adopted to define its *dupA* status.

The *cagA* detection and genotyping of all 248 isolates were performed by PCR tests and subsequent direct sequencing as described previously.²³⁻²⁷

Nucleotide sequence accession numbers

The DNA sequences of the *dupA* region of the 14 representative Japanese strains used in this study were deposited in the DDBJ database under accession numbers AB617832-AB617845; their characteristics are listed in **table 2**. In this study, we refer to the released sequences of 12 *H. pylori* strains whose complete genomes were deposited in GenBank under the following accession numbers: AE001439 for J99, CP001072 for Shi470,

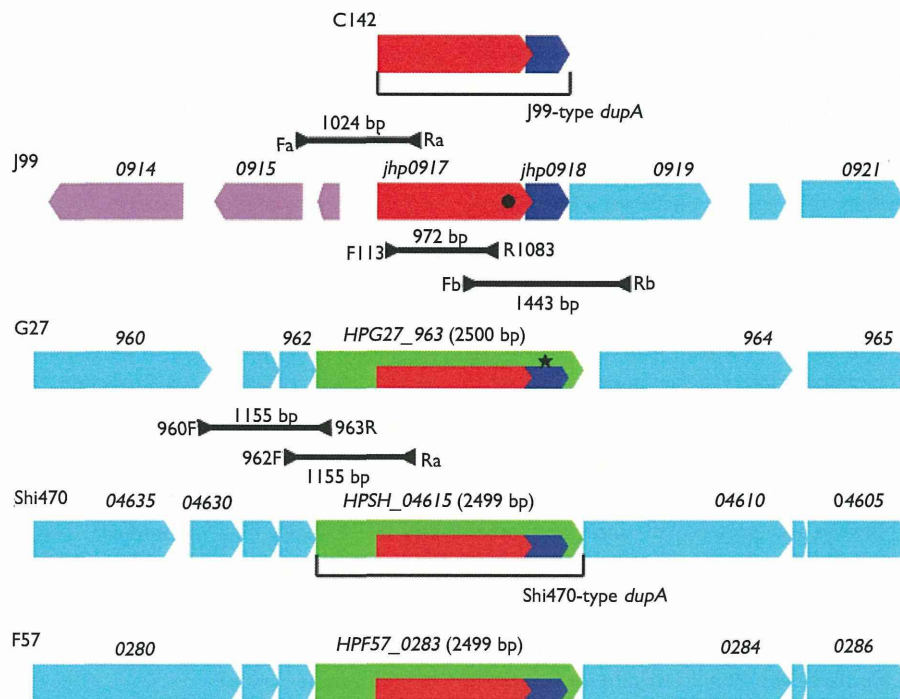


Figure 1. Comparison of the genomic regions surrounding duodenal ulcer-promoting gene A (*dupA*) in 4 published *Helicobacter pylori* (*H. pylori*) genomes and strain C142. The positions of the primers used in this study are also shown.

Sequences of *dupA* (corresponding to *jhp0917* and *jhp0918*) and the surrounding region in the published full-genome sequences of 4 *dupA*⁺ *H. pylori* strains—J99 from the United States, G27 from Italy, Shi470 from a remote Amazonian village in Peru, and F57 from Japan—and strain C142 from Colombia are shown. Initially, *dupA* was reported in J99 as a 1839 bp gene consisting of *jhp0917* and *jhp0918* genes and was found to contain a 1 bp insertion at the 3' end of *jhp0917*, which J99 lacked (indicated by a black dot). Lu et al. found *dupA* of C142 to be a representative gene.²⁷ In strains Shi470 and F57, the sequences corresponding to *dupA* (*jhp0917* and *jhp0918*) were parts of continuous 2499 bp genes, which were highly homologous to each other (*HP_04615* and *HPF57_0283*, respectively). *HPG27_963*, a 2500 bp sequence in strain G27, was homologous to both *HP_04615* and *HPF57_0283* but contained a stop codon created by a 1-bp insertion of a “T” after position 1176, leading to truncation of the gene product (indicated by a black star). In this study, *jhp0917* and *jhp0918* with the described 1 bp insertion was defined as the J99-type *dupA* (indicated by red and blue boxes) and *HPSH_04615* as the Shi470-type *dupA* (indicated by a green box). In J99, the upstream region of *dupA* was completely different from those of the 3 other strains with a full published genome. The nucleotide sequences surrounding Shi470-type *dupA* of Shi470, F57, and G27 were homologous. In the present study, 5 primer pairs were designed to confirm the positivity of *dupA* and consequently classify the genotype of *dupA* as either the J99 or Shi470 type.

CP001173 for G27, CP002076 for Cuz20, CP002184 for HP 908, CP002332 for Gambia 94/24, CP002336 for SouthAfrica7, AP011945 for F57, CP002571 for HP 2017, CP002572 for HP 2018, CP002982 for Puno135, and CP002983 for SNT49. We also refer to the *dupA* sequence of strains C142 (GenBank accession number AB196363; **Fig. 1**), and AB21 (GenBank accession number GU932735).

Statistical analysis

The associations of *dupA* prevalence with clinical diagnosis, geographic locations, and *cagA* genotypes were examined using the Fisher's exact probability test for univariate analysis, and multivariable logistic regression for multivariable analysis. In the multivariable logistic regression, *dupA* positivity was used as a dependent variable and the other 3 as independent variables. All tests were 2-sided, and a probability level (P) of <0.05 was considered significant. All statistical analyses were performed using IBM SPSS Statistics 20 (SPSS Inc., Chicago, IL, USA).

Results

Association between *dupA* and clinical outcomes or *cagA* status

Among the 111 tested strains from Fukui, 24 (21.6%) were positive for both *jhp0917* and *jhp0918* on the dot-blot hybridization, while 22 (19.8%) were positive for both DupAF113/R1083 and DupAFb/Rb according to the PCR test. Accordingly, these strains were defined as *dupA*⁺ on each test. For the dot-blot hybridization, 2 strains were positive for both *jhp0917* and *jhp0918*, but were finally revealed to be *dupA*⁻ by the PCR. One strain was considered *dupA*⁻ because it was *jhp0917*⁺ but *jhp0918*⁻ on the dot-blot hybridization and was confirmed as *dupA*⁻ based on the PCR results. In Okinawa, no strains showed opposite results between the dot-blot hybridization and the PCR tests. The findings were consistent between these 2 tests, with 38 (27.7%) of the 137 tested Okinawan strains defined as *dupA*⁺. The overall agreement between the dot-blot hybridization and the PCR results was 98.2% (109/111) in Fukui and 100% (137/137) in Okinawa, respectively. Combining the results of the

Table 1 Oligonucleotide primers used in this study

Primer	Primer sequence (5'→3')	Reference
DupAFI13	GACGATTGAGCGATGGGAATAT	Argent et al. (2007)
DupAR1083	CTGAGAAGCCTTATTATCTTGTGG	Argent et al. (2007)
DupAFa	TCCCAAATGCTTTGCCTGCG	Present study
DupARa	GCGCTCTGTCAGTAGAAACC	Present study
DupAFb	TGAGCGTGGTAGCTCTTGAC	Present study
DupARb	TCGCTTACAATCCTACCTAGCC	Present study
DupA960F	CCTGAGCCTGTGAATAAACCTG	Present study
DupA963R	ATATGGCGTGGTCTATTGGTG	Present study
DupA962F	GTGTAGCCACCTCTTCTTATC	Present study
JHP0917 (+)	TGGTTTCTACTGACAGAGCGC	Lu et al. (2005)
JHP0917 (-)	AACACGCTGACAGGACAATCTCCC	Lu et al. (2005)
JHP0918-1F	CTCAAGCTAGAAAGATCAACGG	Present study
JHP0918-1R	ACTCTTCTTATAAGTTTCTTGG	Present study

Table 2 Characteristics of the sequenced strains

<i>H. pylori</i> strain	Origin	Disease	<i>cagA</i> genotype	<i>dupA</i> genotype	<i>dupA</i> size (bp)	<i>dupA</i> null mutation
F51	Fukui	DU	East Asian	Shi470	2499	-
F57	Fukui	GC	East Asian	Shi470	2499	-
F58	Fukui	Gastritis	East Asian	Shi470	2499	-
F64	Fukui	DU	East Asian	Shi470	2499	-
F77	Fukui	GU	East Asian	Shi470	2499	-
F80	Fukui	Gastritis	Hybrid	J99	1840	+
F228	Fukui	GC	East Asian	Shi470	2499	-
OK99	Okinawa	DU	East Asian	Shi470	2499	-
OK108	Okinawa	GU	East Asian	Shi470	2499	+
OK165	Okinawa	Gastritis	East Asian	Shi470	2499	-
OK169	Okinawa	DU	East Asian	Shi470	2499	-
OK203	Okinawa	Gastritis	Western	Shi470	2499	-
OK303	Okinawa	GC	East Asian	Shi470	2499	-
OK309	Okinawa	GC	East Asian	Shi470	2499	-
OK317	Okinawa	Gastritis	East Asian	J99	1840	+

H. pylori, *Helicobacter pylori*; *cagA*, cytotoxin-associated gene A; *dupA*, duodenal ulcer-promoting gene A; DU, duodenal ulcer; GC, gastric cancer; GU, gastric ulcer.

dot-blot hybridization and the PCR, the *dupA* status of Fukui and Okinawa were determined.

Twenty-two (19.8%) *dupA*⁺ strains were found in Fukui. The frequency was higher in strains from patients with DU (7/20, 35.0%) than in those from patients with GU (3/20, 15.0%), chronic gastritis (6/39, 15.4%), or GC (6/32, 18.8%). The *dupA* gene was positive in 38 strains (27.7%) isolated in Okinawa, and the prevalence was greater among strains from patients with GC (14/33, 42.4%) than in those with DU (5/26, 19.2%), GU (5/18, 27.8%), or chronic gastritis (14/60, 23.3%). However, no statistical significance between the *dupA* status and clinical outcomes was observed in both areas (Table 3). Further, no association was observed between the *dupA* status and GC histology, with the intestinal and diffuse types observed in both areas (data not shown).

We also determined the *cagA* genotypes. Two strains of F80 (*dupA*⁺) and OK204 (*dupA*⁻) carried the East Asian-type

CagA motif (AB'DD and ABD, respectively) but were assigned as Western in origin on the basis of our previous phylogenetic analysis of *cagA* and were considered a hybrid type. Both F80 and OK 204 were isolated from DU patients. Another strain (OK181) isolated from an Okinawan host with chronic gastritis could not be classified owing to the lack of a *CagA* C/D motif, but was assigned as a Western type by phylogenetic analysis. Consistent with our previous reports,²³ a variety of genotypes was observed for *cagA* among the 137 *H. pylori* strains in Okinawa, including 110 (80.3%) strains with East Asian-type *cagA*, 20 (14.6%) with Western-type *cagA*, 6 (4.4%) *cagA*⁻ strains, and 1 (0.7%) with hybrid-type *cagA*. In contrast, almost all strains in Fukui (109/111, 98.2%) possessed East Asian-type *cagA*, only 1 (0.9%) carried Western-type *cagA*, and none were *cagA*⁻. One (0.9%) strain with hybrid-type *cagA* was also detected in Fukui. This observed high *cagA* prevalence in Japan was also consistent with previous reports.^{47,48}

Next, we focused on the relationship between *dupA* and *cagA* statuses for *H. pylori*. We measured the *dupA* prevalence of *H. pylori* strains with East Asian-*cagA*, the most dominant *cagA* genotype in Japan, against those with non-East Asian *cagA* status (i.e., the combination of Western-type *cagA*⁺ and *cagA*⁻ strains). The 2 strains with hybrid-type *cagA* were excluded from this analysis due to the association between *dupA* and *cagA*. In Okinawa, only 1 *cagA*⁻ strain (3.8%) of the 26 Western-type *cagA* or *cagA*⁻ strains was *dupA*⁺. In contrast, 37 (33.6%) of the 110 Okinawan strains with the East Asian-type *cagA* carried *dupA* ($p=0.0013$)(Table 4). The relationship of *dupA* and *cagA* statuses could not be assessed in Fukui because of the extremely small number of *H. pylori* strains with non-East Asian *cagA* status.

In the 246 tested Japanese strains isolated from both Fukui and Okinawa (excluding F80 and OK204), the associations of *dupA* prevalence with clinical diagnosis, geographic locations, and *cagA* genotypes were analyzed (Table 5). In the univariate analysis, only East Asian-*cagA* positivity was related to the presence of *dupA* (26.5% vs. 3.7%, $p=0.0073$). In the multivariate analysis, strains isolated from Okinawa and those with East Asian-type *cagA* positivity were significantly associated with an increased probability for *dupA* positive status (odds ratio [OR]=2.128, 95% confidence interval [CI]=1.146-3.949 and OR=12.924, 95% CI=1.689-98.901, respectively). No significant association was found between any tested clinical diagnosis and *dupA* status in both statistical analyses.

Comparison of *dupA* sequences and the upstream region between genome-sequenced reference strains

We first compared *dupA* sequences (corresponding to *jhp0917* and *jhp0918*) and the upstream region between the released genome sequences from 3 *dupA*⁺ *H. pylori* strains (Shi470, G27, and J99). In strain Shi470, the sequence corresponding to *dupA* (*jhp0917* and *jhp0918*) was part of a continuous 2499 bp gene, *HP_04615*. *HPG27_963* is a 2500 bp sequence from strain G27, which was isolated from Italy and was homologous to *HP_04615*; however, *HPG27_963* contained a stop codon, resulting in the truncation of this gene product. In J99, the upstream region of *dupA* was entirely different from those of the other 2 strains. In the genome sequences of J99, the direction of *jhp0917*, *jhp0918*, and the downstream genes was opposite to that of *jhp0916*, *jhp0915*, and *jhp0914*, while the series of genes centered by *HP_04615* and *HPG27_963* were aligned in the same direction in the partial genome sequences of Shi470 and G27, respectively (Fig. 1). Thus, we hypothesized the “original” *dupA* reported by Lu et al. may be the legacy of a truncated gene that resulted from the deletion of the 5' region of the full-length *dupA*. Here, we sub-classified *dupA* into 2 genotypes by defining *jhp0917* and *jhp0918* as J99-type *dupA* and *HPSH_04615* as Shi470-type *dupA*. On the basis of these results, a chromosomal alignment was performed from 12 released *H. pylori* genome sequences available in the public database GenBank as of February 2012. Seven strains (Shi470, G27, Cuz20, SouthAfrica7, F57, Puno135, and SNT49) were of the Shi470 type, and 5 strains (J99, HP 908, Gambia 94/24, HP 2017, and HP 2018), of the J99 type. Strains HP 2017 and HP 2018 were the chronological subclones of HP 908.⁴⁹ With the exception of G27, the Shi470-type strains carried intact full-

length *dupA* consisting of 2499 bp.

Sub-classification of *dupA* into 2 genotypes

On the basis of the published sequences, 3 primer pairs were designed for PCR to distinguish the 2 *dupA* genotypes (the Shi470 and J99 types) (Table 1 & Fig. 1). All 60 *dupA*⁺ strains in this study (22 from Fukui and 38 from Okinawa) were examined: 58 (96.7%) were of the Shi470 type, 57 were positive for both 960F/963R and 962F/Ra and were of the Shi470 type, 1 strain (OK329) was positive for 962F/Ra but was negative for 960F/963R and was assigned as the Shi470 type, and 2 strains (F80 and OK317) were positive for only Fa/Ra and were classified as the J99 type (Table 2 & Table 6).

Sequence analysis of full-length *dupA* from clinical isolates in Japan

We next examined the sequence diversity of 15 full-length *dupA* from Japanese clinical isolates. We compared 13 Shi470-type Japanese strains (6 from Fukui and 7 from Okinawa), including F57, whose complete genome sequence was recently released. Twelve of these strains (92.3%) carried intact full-length *dupA* (Table 2). Alignments of the nucleotide and amino acid sequences showed these strains were highly homologous (98.9%, standard deviation [SD] ± 0.4) irrespective of the clinical outcome and the area of isolation (Fukui or Okinawa). The remote Amazonian strain Shi470 was also highly homologous to those 13 Japanese strains (98.5%, $SD\pm 0.2$)(Table 7). Sequences from the remaining 2 Japanese strains (F80 and OK317), which carried the J99-type *dupA*, were also compared with the corresponding J99 sequences (1838 bp). These strains were highly homologous to each other (99.9%) but less homologous to J99 (95.7%). A G/T insertion at position 1633, resulting in a null mutation, was found in both strains (Table 2); this mutation was previously reported in a strain from Argentina.⁴⁴ All 15 Japanese strains possessed the 1 bp insertion of a C or T in the 3' region of *jhp0917*, which was initially reported by Lu et al. Recently, Hussein et al. also classified *dupA* into 2 main groups. These investigators reported that *dupA1* was a 1884 bp ORF with a longer 3' end than that initially described by Lu et al. and that *dupA2* was a truncated gene.⁴⁵ To evaluate the correspondence of the Shi470-type *dupA* to *dupA1*, we compared the 13 Shi470-type *dupA* sequences of the Japanese isolates included in the present study, with the *dupA1* sequence of strain AB21 released by Hussein et al. We found all of these sequences included an intact *dupA1* at the 3' end of the gene. OK108, a strain with an incomplete Shi470-type *dupA*, also possessed intact *dupA1* sequences, as the stop codon causing a truncation of the 2499 bp ORF was located upstream of the beginning of the *dupA1* lesion.

Discussion

In this study, we found no significant association between *dupA* and certain diseases in the 2 distant areas in Japan (Fukui and Okinawa) and could confirm no relationship between the *dupA* gene and the lower incidence of GC in Okinawa. However, our results indicated patients infected with *dupA*⁺ strains were prone to DU in Fukui, as opposed to the high frequency of *dupA*⁺ strains

Table 3 Comparison of *dupA* prevalence among *H. pylori* groups with various clinical outcomes in the 2 different areas in Japan

Clinical outcome	<i>dupA</i> prevalence (%)	
	Fukui (n=111)	Okinawa (n=137)
Duodenal ulcer	7/20 (35.0)	5/26 (19.2)
Gastric ulcer	3/20 (15.0)	5/18 (27.8)
Chronic gastritis	6/39 (15.4)	14/60 (23.3)
Gastric cancer	6/32 (18.8)	14/33 (42.4)
Total	22/111 (19.8)	38/137 (27.7)

H. pylori, *Helicobacter pylori*; *dupA*, duodenal ulcer-promoting gene A.

Table 4 Relationship between *dupA* prevalence and the *cagA* genotype

<i>cagA</i> genotype	<i>dupA</i> prevalence (%)	
	Fukui	Okinawa
East Asian	21/109 (19.3)	37/110 (33.6)
Western and <i>cagA</i> ⁻	0/1 (0.0)	1/26 (3.8)

In Okinawa, *dupA* positivity was significantly higher in the East Asian-type *cagA*⁺ strains than in the Western-type *cagA*⁺ and *cagA*⁻ strains (P=0.0013, Fisher's exact probability test). Two stains isolated from duodenal ulcer hosts with hybrid-type *cagA*, F80 (*dupA*⁺) and OK204 (*dupA*⁻), were excluded. *cagA*, cytotoxin-associated gene A; *dupA*, duodenal ulcer-promoting gene A.

Table 5 The associations of *dupA* prevalence with clinical diagnosis, geographic locations, and *cagA* genotypes

	<i>dupA</i> positivity (%)	Univariate ^a p value	Multivariate ^b	
			OR (95% CI)	p value
Disease				
Chronic gastriti	20/99 (20.2)	Referent	–	0.472
Gastric ulcer	8/38 (21.1)	1.0000	–	0.272
Duodenal ulcer	11/44 (25.0)	0.5177	–	0.295
Gastric cancer	20/65 (30.8)	0.1395	–	0.167
Geography				
Okinawa	38/136 (27.9)	0.1330	2.128 (1.146–3.949)	0.017
Fukui	21/110 (19.1)			
<i>cagA</i> genotype				
East Asian	58/219 (26.5)	0.0073	12.924 (1.689–98.901)	0.014
Non-East Asian	1/27 (3.7)			

Two stains isolated from duodenal ulcer hosts with hybrid-type *cagA*, F80 (*dupA*⁺) and OK204 (*dupA*⁻), were excluded. *dupA*, duodenal ulcer-promoting gene A; OR, odds ratio; CI, confidence interval; *cagA*, cytotoxin-associated gene A; a Fisher's exact probability test; b multivariable logistic regression.

Table 6 Distribution of *dupA* genotypes in clinical strains

	Prevalence (%)		
	Fukui (n=22)	Okinawa (n=38)	Total (n=60)
J99-type	1 (4.5)	1 (2.6)	2 (3.3)
Shi470-type	21 (95.5)	37 (97.4)	58 (96.7)

dupA, duodenal ulcer-promoting gene A.

among patients with GC in Okinawa. In a systematic review, Hussein reported *dupA* promotes DU in some populations and GU and GC in others.⁵⁰ Meanwhile, based on a meta-analysis, Shiota et al. reported the importance of *dupA* positivity in DU pathogenesis, especially in Asian countries.⁵¹ These conflicting results probably result from differences in the circulating *H. pylori* strains between East Asia and the West. Although the mechanism by which *H. pylori* is involved in 2 extremely different gastroduodenal diseases (DU and GC) remains unclear, our discrepant results in 2 different areas in Japan suggest *dupA* may be one of the virulence determinants that causes severe diseases, while other virulence factors, host differences, and environmental factors might affect the clinical outcome of the infection. Fukui is a typical rural prefecture located on the central Japanese mainland (Honshu), while Okinawa consists of islands in the southwestern part of Japan. Historically, Okinawa has had more

active international communication than the rest of the country. Because these geographical and historical factors may affect the development of gastroduodenal diseases in Okinawan hosts, the pathogenesis of *H. pylori* isolated from Okinawa needs to be analyzed more comprehensively.

Seven studies have investigated the association of *dupA* with *cagA*, one of the most widely studied virulence genes, but the results have been inconsistent. A positive association between the *dupA* and *cagA* statuses was reported in a study investigating strains isolated from patients with chronic gastritis or DU in North India,³¹ whereas 3 other studies refuted the presence of a relationship with any clinical outcomes in China,³⁷ Iraq, and Iran.^{35,42} Douraghi et al. reported *dupA* was associated with *cagA* only in patients with DU in Iran.³⁴ A Brazilian study also reported the association of these 2 genes was limited to a group of strains from adult hosts with DU.³³ Argent et al. investigated the

Table 7 Analysis of divergence of the Shi470-type *dupA*

Strain	Nucleotide and amino acid identity* (%)													
	Shi470	F51	F57	F58	F64	F77	F228	OK99	OK108 ^b	OK165	OK169	OK203	OK303	OK309
Shi470		98.2	98.8	99.0	99.0	98.3	98.9	98.3	–	98.1	98.1	98.4	98.8	98.2
F51	98.3		98.2	98.2	98.2	98.0	98.3	97.7	–	97.7	97.6	97.8	98.2	97.6
F57	98.6	98.4		99.0	99.0	98.8	99.4	98.8	–	98.8	98.8	99.2	99.3	98.9
F58	98.8	98.4	98.7		100	98.6	99.2	98.8	–	98.6	98.3	98.7	99.0	98.4
F64	98.8	98.4	98.7	100		98.6	99.2	98.8	–	98.6	98.3	98.7	99.0	98.4
F77	98.7	98.6	99.0	98.8	98.8		98.7	99.0	–	98.3	98.1	98.4	98.6	98.2
F228	98.8	98.4	99.4	98.8	98.8	98.9		98.7	–	98.7	98.7	99.0	99.6	98.8
OK99	98.5	98.2	98.8	98.9	98.9	99.1	98.8		–	98.6	98.1	98.4	98.4	98.2
OK108 ^b	98.5	98.2	99.2	99.1	99.1	98.9	99.2	98.4		–	–	–	–	–
OK165	98.5	98.5	98.9	98.9	98.9	99.0	98.9	99.3	98.6		99.3	99.4	98.6	99.4
OK169	98.2	98.2	99.0	98.3	98.3	98.6	99.1	98.6	98.7	99.2		99.6	98.6	99.9
OK203	98.3	98.3	99.1	98.5	98.5	98.8	99.2	98.7	98.9	99.2	99.8		98.9	99.8
OK303	98.7	98.4	99.4	98.8	98.8	98.9	98.8	98.8	99.2	98.9	99.1	99.2		98.7
OK309	98.2	98.2	99.0	98.4	98.4	98.7	99.1	98.6	98.8	99.2	100	99.8	99.1	

dupA, duodenal ulcer-promoting gene A; a values below and above the diagonal represent nucleotide and amino acid sequence, respectively; b a stop codon is present in the *dupA* nucleotide sequence.

dupA prevalence in *H. pylori* strains from Belgium, South Africa, China, and the United States. These investigators reported a significant association between *dupA* positivity with GC, independent of *cagA* status.³² We previously showed that more than 20% of Okinawan strains were either Western-type *cagA*⁺ or *cagA*⁻, both of which were rare in East Asia.²³ We also found these Western-type strains were isolated among patients with DU more frequently than the East Asian strains,^{26,27} whereas the East Asian-type strains in Okinawa were associated with GC.²⁷ Therefore, we examined the association between *dupA* and *cagA* status in Okinawa. Intriguingly, we found a low prevalence of the *dupA*⁺ strain among strains with the non-East Asian *cagA* (the Western or hybrid type) in Okinawa. Moreover, both univariate and multivariate analyses showed that the presence of East Asian-type *cagA* was significantly associated with *dupA* positivity. Although the reason why *dupA*⁺ strains are rare among non-East Asian *cagA*⁺ strains is unclear, the variety in *cagA* toxicity may partially, if not completely, explain this mystery. Hussein et al. reported that strains with *cagA* genes encoding more than 3 tyrosine phosphorylation motifs of the Src homology phosphatase 2 (SHP-2) binding site were significantly associated with *dupA* positivity when compared to strains with only 3 phosphorylation motifs in Iran.³⁵ The virulence of *cagA*, which is determined by the degree of CagA SHP-2 binding activity, depends on the genotypes of the SHP-2 binding site (the East Asian-type is more toxic than the Western-type) and the number of its phosphorylation motifs (the greater the number of motifs, the stronger the binding).^{22,25,27,52} Together, the results of Hussein et al. and those of our present study suggest the possible association of *dupA* with “toxic” *cagA*.

We found that the *dupA* prevalence in Okinawa was significantly higher than in Fukui by using multivariable logistic regression. This result seems partially consistent with those of recent meta-analyses showing that the prevalence of *dupA* is higher in Western countries than in Asian countries,^{50,51} as our previous reports suggested *H. pylori* strains in Okinawa may have had a greater opportunity for the transfer of DNA from Western

countries than *H. pylori* strains in other Japanese areas.^{23,26} Since this question has not been sufficiently studied, determining the genetic origin of *H. pylori* strains circulating in Okinawa is required in examining the roles of *H. pylori* virulent factors, including *dupA*, in this area.

In this study, we analyzed the upstream nucleotide sequences of *dupA* in Japanese clinical *H. pylori* isolates, which have not been sufficiently examined in Japan thus far. A comparison between the genome sequences of 12 representative *dupA*⁺ strains of *H. pylori* in GenBank, including our strain (F57), revealed the existence of 2 major distinct chromosomal arrangements (Shi470 and J99 types). Regardless of the host’s clinical outcome, we showed that most *dupA* sequences of the Japanese *H. pylori* strains were of the intact Shi470-type gene, which encodes a protein of 832 amino acids. Although this finding made it difficult to determine if *dupA* was a specific virulence factor in Japan, we demonstrated a strong association between intact *dupA* and *H. pylori* strains circulating in this country. When discussing the virulence of a particular *H. pylori* gene, it is important to consider not only the presence of the gene but also whether the gene is intact. We previously showed *vacA* from half of the Japanese non-cytotoxic strains contained null mutations resulting in a lack of VacA activity.³³ In terms of *dupA*, Queiroz et al. reported an inverse association between the presence of *dupA* without particular null mutations (a deletion of adenine at position 1311 and insertion of adenine at position 1426) and the development of GC in Brazil.⁴¹

Notably, Hussein et al. had classified *dupA* into 2 main groups (*dupA1* and *dupA2*) before us. This group reported *dupA1* is the most common genotype, as well as the active form that induces host secretion of IL-12 from cluster of differentiation 14 (CD14) positive mononuclear cells. Among the 25 *dupA1*⁺ isolates studied by Hussein et al., additional sequencing was performed for 2 isolates. Surprisingly, these isolates possessed the *dupA* gene with an extended 5’ end, giving a total length of 2499 bp.⁴⁵ Because all 13 Shi470-type *dupA* strains sequenced

in this study included the 1884bp dupA1 defined by Hussein et al., dupA1 may be longer than initially reported, corresponding to the Shi470-type dupA in the present study. On the other hand, we cannot deny the possibility the Shi470-type dupA is a third novel genotype of dupA, different from both dupA1 and dupA2. Following Hussein et al., Queiroz et al. sequenced the complete dupA gene from 6 *H. pylori* isolates in Brazil. Though all these genes were reported to be identical to dupA1, the report did not specify whether the 5' end was extensive or not.⁴⁶ For assessing the correspondence of the Shi470-type dupA to dupA1, further investigations on the upstream region of dupA are required. Investigating the dupA genotype might provide insight into the potential relationship between intact dupA and the strong virulence of *H. pylori* strains.

It should be noted that dupA gene expression has not been sufficiently analyzed thus far. Only 2 of the previous studies on dupA have investigated its expression in various isolates, as determined by reverse transcription PCR (RT-PCR). In Japan, Nguyen et al. confirmed dupA expression in all 10 randomly selected *H. pylori* strains among 72 dupA⁺ isolates.³⁹ Only recently, Alam et al. reported a significant association of dupA with DU development in a South Indian population.⁴⁵ They also reported the detection of dupA transcription in 28 of 35 dupA⁺ *H. pylori* strains. The discovery of strains with “expressive dupA” by RT-PCR and an assessment of their relationship with clinical outcomes would reveal the true role of the DupA protein in the disease development of the host. Therefore, we should next assess the dupA expression of the Japanese isolates used in the present study, especially the Shi470-type dupA⁺ isolates, by using the methods of Alam et al. Furthermore, the detection of DupA protein still remains an unsolved problem.³⁰

Further exploration of the surrounding genes of dupA may also be promising for understanding *H. pylori* virulence. Previous studies have shown that dupA is present in the plasticity zone. This zone is characterized by a low G+C content and an abundance of strain-specific ORFs, including TFSSs.^{11,28,29} Recently, Kersulyte et al. described a putative T4SS-containing dupA as a type IV secretion 3a (*tfs3a*) gene, and a putative T4SS-containing a *virB4*

sequence, but not dupA as *tfs3b*.²⁹ Jung et al. defined the presence of dupA and all 6 adjacent virulence (*vir*) gene homologs (*virB8*, *B9*, *B10*, *B11*, *virD4*, and *D2*) as a complete dupA cluster.³⁰ They reported that the presence of a complete dupA cluster but not dupA alone is associated with DU development in the United States population. Because we could not find a particular association between dupA and any clinical outcomes, the *vir* genes around dupA in the Japanese *H. pylori* isolates studied in the present study will need to be researched further.

In conclusion, we were unable to confirm a close association between dupA and clinical outcomes in 2 areas in Japan with different GC risks. However, we found intact dupA consists of a 2499 bp sequence and most Japanese dupA⁺ strains possess the intact genotype. We also discovered a significant relation between the presence of dupA and the East Asian-type *cagA* in Japan. In addition, dupA positivity was independently associated with strains isolated from Okinawa.

Further global analyses of the genetic structure of dupA and the association between the *H. pylori* strain with a dupA-positive state and clinical outcomes are required.

Contributors

Hidetaka Matsuda, Yoshiyuki Ito, Hiroyuki Suto, Satoko Satomi, Masahiro Ohtani, Yukinao Yamazaki, Yoshiki Shimabukuro, Kaoru Kikuchi, Yoshihide Keida, Takeshi Azum, and Yasunari Nakamoto were involved in conceiving and designing this study. Hidetaka Matsuda, Yoshiyuki Ito, and Akiyo Yamakawa analyzed and interpreted the data. Yukinori Kusaka supervised and revised the statistics. This manuscript was drafted by Hidetaka Matsuda, revised critically by Yoshiyuki Ito for important intellectual content, and finalized by Yasunari Nakamoto with the assistance of all authors.

Conflicts of interest

The authors declared no conflicts of interest.

Summary Box

What is already known:

- The association between duodenal ulcer-promoting gene A (*dupA*) of *Helicobacter pylori* (*H. pylori*) and various clinical outcomes or other virulence factors remains controversial.
- In Japan, Okinawa has lowest incidence of gastric cancer (GC). The diversity of cytotoxin-associated gene A (*cagA*) detected in Okinawa includes both East Asian and Western genotypes and is an important factor for the low prevalence of GC.
- *dupA* is reported to be polymorphic; *dupA1* (1884 bp) is the active form, while *dupA2* is the truncated version. Several *H. pylori* strains are reported to possess long *dupA1* sequences (2499 bp) because of an extended 5' end.

What the new findings are:

- We found *dupA* could be classified into 2 genotypes—a 2499 bp genotype and the initially reported 1839 bp genotype. These genotypes were designated Shi470-type *dupA* and J99-type *dupA*, respectively, after the *H. pylori* strains whose complete genomes have been released.
- In Japan, most dupA⁺ *H. pylori* strains possess intact Shi470-type *dupA*.
- In Japan, *dupA* appeared to be independently associated with the East Asian-type *cagA* and with host residence in Okinawa.

References

- Marshall BJ, Goodwin CS, Warren JR, et al. Prospective double blind-trial of duodenal ulcer relapse after eradication of *Campylobacter pylori*. *Lancet* 1988; 2(8626):1437-42.
- Parsonnet J, Friedman GD, Vandersteen DP, et al. *Helicobacter pylori* infection and the risk of gastric carcinoma. *N Engl J Med* 1991; 325(16):1127-31.
- Wotherspoon AC, Ortiz-Hidalgo C, Falzon MR, et al. *Helicobacter pylori*-associated gastritis and primary B-cell gastric lymphoma. *Lancet* 1991; 338(8776):1175-6.
- Blaser MJ, Perez-Perez GI, Kleanthous H, et al. Infection with *Helicobacter pylori* strains possessing *cagA* is associated with an increased risk of developing adenocarcinoma of the stomach. *Cancer Res* 1995; 55(10):2111-5.
- Parsonnet J, Friedman GD, Orentreich N, et al. Risk for gastric cancer in people with CagA positive or CagA negative *Helicobacter pylori* infection. *Gut* 1997; 40(3):297-301.
- Stephens JC, Stewart JA, Folwell AM, et al. *Helicobacter pylori cagA* status, *vacA* genotypes and ulcer disease. *Eur J Gastroenterol Hepatol* 1998; 10(5):381-4.
- Hamlet A, Thoreson AC, Nilsson O, et al. Duodenal *Helicobacter pylori* infection differs in *cagA* genotype between asymptomatic subjects and patients with duodenal ulcers. *Gastroenterology* 1999; 116(2):259-68.
- Rugge M, Busatto G, Cassaro M, et al. Patients younger than 40 years with gastric carcinoma: *Helicobacter pylori* genotype and associated gastritis phenotype. *Cancer* 1999; 85(12):2506-11.
- Atherton JC, Cao P, Peek RM Jr, et al. Mosaicism in vacuolating cytotoxin alleles of *Helicobacter pylori*. Association of specific *vacA* types with cytotoxin production and peptic ulceration. *J Biol Chem* 1995; 270(30):17771-7.
- Atherton JC, Peek RM Jr, Tham KT, et al. Clinical and pathological importance of heterogeneity in *vacA*, the vacuolating cytotoxin gene of *Helicobacter pylori*. *Gastroenterology* 1997; 112(1):92-9.
- Yamaoka Y. Roles of the plasticity regions of *Helicobacter pylori* in gastroduodenal pathogenesis. *J Med Microbiol* 2008; 57(5):545-53.
- Wen S, Moss SF. *Helicobacter pylori* virulence factors in gastric carcinogenesis. *Cancer Lett* 2009; 282(1):1-8.
- Proença-Modena JL, Acrani GO, Brocchi M. *Helicobacter pylori*: phenotypes, genotypes and virulence genes. *Future Microbiol* 2009; 4(2):223-40.
- Covacci A, Telford JL, Del Giudice G, et al. *Helicobacter pylori* virulence and genetic geography. *Science* 1999; 284(5418):1328-33.
- Falush D, Wirth T, Linz B, et al. Traces of human migrations in *Helicobacter pylori* populations. *Science* 2003; 299(5612):1582-5.
- Linz B, Balloux F, Moodley Y, et al. An African origin for the intimate association between humans and *Helicobacter pylori*. *Nature* 2007; 445(7130):915-8.
- Azuma T. *Helicobacter pylori* CagA protein variation associated with gastric cancer in Asia. *J Gastroenterol* 2004; 39(2):97-103.
- Correa P. A human model of gastric carcinogenesis. *Cancer Res* 1988; 48(13):3554-60.
- Ito S, Azuma T, Murakita H, et al. Profile of *Helicobacter pylori* cytotoxin derived from two areas of Japan with different prevalence of atrophic gastritis. *Gut* 1996; 39(6):800-6.
- Nobuta A, Asaka M, Sugiyama T, et al. *Helicobacter pylori* infection in two areas in Japan with different risks for gastric cancer. *Aliment Pharmacol Ther* 2004; 20 (Suppl 1):1-6.
- Ito Y, Azuma T, Ito S, et al. Sequence analysis and clinical significance of the *iceA* gene from *Helicobacter pylori* strains in Japan. *J Clin Microbiol* 2000; 38(2):483-8.
- Azuma T, Yamakawa A, Yamazaki S, et al. Correlation between variation of the 3' region of the *cagA* gene in *Helicobacter pylori* and disease outcome in Japan. *J Infect Dis* 2002; 186(11):1621-30.
- Zhou W, Yamazaki S, Yamakawa A, et al. The diversity of *vacA* and *cagA* of *Helicobacter pylori* in East Asia. *FEMS Immunol Med Microbiol* 2004; 40(1):81-7.
- Azuma T, Yamakawa A, Yamazaki S, et al. Distinct diversity of the *cag* pathogenicity island among *Helicobacter pylori* strains in Japan. *J Clin Microbiol* 2004; 42(6):2508-17.
- Azuma T, Yamazaki S, Yamakawa A, et al. Association between diversity in the Src homology 2 domain-containing tyrosine phosphatase binding site of *Helicobacter pylori* CagA protein and gastric atrophy and cancer. *J Infect Dis* 2004; 189(5):820-7.
- Yamazaki S, Yamakawa A, Okuda T, et al. Distinct diversity of *vacA*, *cagA*, and *cagE* genes of *Helicobacter pylori* associated with peptic ulcer in Japan. *J Clin Microbiol* 2005; 43(8):3906-16.
- Satomi S, Yamakawa A, Matsunaga S, et al. Relationship between the diversity of *cagA* gene of *Helicobacter pylori* and gastric cancer in Okinawa, Japan. *J Gastroenterol* 2006; 41(7):668-73.
- Lu H, Hsu PI, Graham DY, et al. Duodenal ulcer promoting gene of *Helicobacter pylori*. *Gastroenterology* 2005; 128(4):833-48.
- Kersulyte D, Lee W, Subramaniam D, et al. *Helicobacter pylori*'s plasticity zones are novel transposable elements. *PLoS One* 2009; 4(9):e6859.
- Jung SW, Sugimoto M, Shiota S, et al. The intact *dupA* cluster is a more reliable *Helicobacter pylori* virulence marker than *dupA* alone. *Infect Immun* 2012; 80(1):381-7.
- Arachchi HS, Kalra V, Lal B, et al. Prevalence of duodenal ulcer-promoting gene (*dupA*) of *Helicobacter pylori* in patients with duodenal ulcer in North Indian population. *Helicobacter* 2007; 12(6):591-7.
- Argent RH, Burette A, Miendje Deyi VY, et al. The presence of *dupA* in *Helicobacter pylori* is not significantly associated with duodenal ulceration in Belgium, South Africa, China, or North America. *Clin Infect Dis* 2007; 45(9):1204-6.
- Gomes LI, Rocha GA, Rocha AM, et al. Lack of association between *Helicobacter pylori* infection with *dupA*-positive strains and gastroduodenal diseases in Brazilian patients. *Int J Med Microbiol* 2008; 298(3-4):223-30.
- Douraghi M, Mohammadi M, Oghalaie A, et al. *dupA* as a risk determinant in *Helicobacter pylori* infection. *J Med Microbiol* 2008; 57(5):554-62.
- Hussein NR, Mohammadi M, Talebkhan Y, et al. Differences in virulence markers between *Helicobacter pylori* strains from Iraq and those from Iran: potential importance of regional differences in *H. pylori*-associated disease. *J Clin Microbiol* 2008; 46(5):1774-9.
- Pacheco AR, Proença-Módena JL, Sales AI, et al. Involvement of the *Helicobacter pylori* plasticity region and *cag* pathogenicity island genes in the development of gastroduodenal diseases. *Eur J Clin Microbiol Infect Dis* 2008; 27(11):1053-9.
- Zhang Z, Zheng Q, Chen X, et al. The *Helicobacter pylori* duodenal ulcer promoting gene, *dupA* in China. *BMC Gastroenterol* 2008; 8:49.
- Schmidt HM, Andres S, Kaakoush NO, et al. The prevalence of the duodenal ulcer promoting gene (*dupA*) in *Helicobacter pylori* isolates varies by ethnic group and is not universally associated with disease development: a case-control study. *Gut Pathog* 2009; 1(1):5.
- Nguyen LT, Uchida T, Tsukamoto Y, et al. *Helicobacter pylori dupA* gene is not associated with clinical outcomes in the Japanese population. *Clin Microbiol Infect* 2010; 16(8):1264-9.
- Imagawa S, Ito M, Yoshihara M, et al. *Helicobacter pylori dupA* and gastric acid secretion are negatively associated with gastric cancer development. *J Med Microbiol* 2009; 59(12):1484-9.
- Queiroz DM, Rocha GA, Rocha AM, et al. *dupA* polymorphisms and risk of *Helicobacter pylori*-associated diseases. *Int J Med Microbiol* 2011; 301(3):225-8.
- Abadi AT, Taghvaei T, Wolfram L, et al. Infection with *Helicobacter pylori* strains lacking *dupA* is associated with an increased risk of gastric ulcer and gastric cancer development. *J Med Microbiol* 2012; 61(1):23-30.
- Alam J, Maiti S, Ghosh P, et al. Significant association of *dupA* of *Helicobacter pylori* with duodenal ulcer development in South East Indian population. *J Med Microbiol* 2012; 61(Pt 9):1295-302.
- Matteo MJ, Armitano RI, Granados G, et al. *Helicobacter pylori oipA*, *vacA* and *dupA* genetic diversity in individual hosts. *J Med Microbiol* 2010; 59(1):89-95.
- Hussein NR, Argent RH, Marx CK, et al. *Helicobacter pylori dupA* is polymorphic, and its active form induces proinflammatory cytokine secretion by mononuclear cells. *J Infect Dis* 2010; 202(2):261-9.
- Queiroz DM, Moura SB, Rocha AM, et al. The genotype of the Brazilian *dupA*-positive *Helicobacter pylori* strains is *dupA1*. *J Infect Dis* 2011; 203(7):1033-4.
- Ito Y, Azuma T, Ito S, et al. Analysis and typing of the *vacA* gene from *cagA*-positive strains of *Helicobacter pylori* isolated in Japan. *J Clin Microbiol* 1997; 35(7):1710-4.
- Mizushima T, Sugiyama T, Komatsu Y, et al. Clinical relevance of the *babA2* genotype of *Helicobacter pylori* in Japanese clinical isolates. *J Clin Microbiol* 2001; 39(7):2463-5.
- Avasthi TS, Devi SH, Taylor TD, et al. Genomes of two chronological isolates (*Helicobacter pylori* 2017 and 2018) of the West African *Helicobacter pylori* strain 908 obtained from a single patient. *J Bacteriol* 2011; 193(13):3385-6.
- Hussein NR. The association of *dupA* and *Helicobacter pylori*-related gastroduodenal diseases. *Eur J Clin Microbiol Infect Dis* 2010; 29(7):817-21.
- Shiota S, Matsunari O, Watada M, et al. Systematic review and meta-analysis: the relationship between the *Helicobacter pylori dupA* gene and clinical outcomes. *Gut Pathog* 2010; 2(1):13.
- Higashi H, Tsutsumi R, Fujita A, et al. Biological activity of the *Helicobacter pylori* virulence factor CagA is determined by variation in the tyrosine phosphorylation sites. *Proc Natl Acad Sci USA* 2002; 99(22):14428-33.
- Ito Y, Azuma T, Ito S, et al. Full-length sequence analysis of the *vacA* gene from cytotoxic and noncytotoxic *Helicobacter pylori*. *J Infect Dis* 1998; 178(5):1391-8.

ORIGINAL ARTICLE

Membrane-bound form of monocyte chemoattractant protein-1 enhances antitumor effects of suicide gene therapy in a model of hepatocellular carcinoma

Y Marukawa¹, Y Nakamoto¹, K Kakinoki¹, T Tsuchiyama¹, N Iida¹, T Kagaya¹, Y Sakai¹, M Naito², N Mukaida³ and S Kaneko¹

Suicide gene therapy using the herpes simplex virus thymidine kinase/ganciclovir (HSV-tk/GCV) system combined with monocyte chemoattractant protein-1 (MCP-1) provides significant antitumor efficacy. The current study was designed to evaluate the antitumor immunity of a newly developed membrane-bound form of MCP-1 (mMCP-1) in an immunocompetent mouse model of hepatocellular carcinoma (HCC). A recombinant adenovirus vector (rAd) harboring the human *MCP-1* gene and the membrane-spanning domain of the *CX3CL1* gene was used. Large amounts of MCP-1 protein were expressed and accumulated on the tumor cell surface. The growth of subcutaneous tumors was markedly suppressed when tumors were treated with mMCP-1, as compared with soluble MCP-1, in combination with the HSV-tk/GCV system ($P < 0.01$). The numbers of Mac-1-, CD4- and CD8a-positive cells were significantly higher in tumor tissues ($P < 0.05$), and tumor necrosis factor (TNF) mRNA expression levels with mMCP-1 were almost five-fold higher than those with soluble MCP-1. These results indicate that the delivery of the *mMCP-1* gene greatly enhanced antitumor effects following the apoptotic stimuli by promoting the recruitment and activation of macrophages and T lymphocytes, suggesting a novel strategy of immune-based gene therapy in the treatment of patients with HCC.

Cancer Gene Therapy (2012) 19, 312–319; doi:10.1038/cgt.2012.3; published online 9 March 2012

Keywords: herpes simplex virus thymidine kinase; hepatocellular carcinoma; membrane-bound form; monocyte chemoattractant protein-1; monocyte/macrophages

INTRODUCTION

In spite of the recent development of locoregional treatments for hepatocellular carcinoma (HCC), the frequency of tumor recurrence remains high, probably because of insufficient therapeutic effects and the multicentric development of HCC in cirrhotic liver.^{1–3} Non-surgical treatments of HCC, such as radiofrequency ablation, transcatheter arterial embolization and transcatheter arterial chemotherapy induce apoptosis of HCC cells, but these treatments do not enhance antitumoral immunity sufficiently. Thus, gene therapy aimed at enhancing antitumor immune responses may be a promising approach to prevent HCC recurrence, when it is combined with non-surgical maneuvers.

We previously reported that monocyte chemoattractant protein-1 (*MCP-1*) gene delivery using recombinant adenovirus vector (rAd) *in vivo* can enhance the efficacy of suicide gene therapy consisting of the delivery of rAd containing herpes simplex virus thymidine kinase (HSV-tk) and ganciclovir (GCV) in models of HCC^{4,5} and colon cancer.⁶ We further demonstrated that the antitumor effects depended on the activation of macrophages.^{4,5} The adenovirus-specific spatial and temporal expression pattern may result in the production of the transgene for a limited time.⁷ Mirroring these characteristics, the adenovirus vector-mediated delivery of the *MCP-1* gene alone was not sufficient to reduce tumor growth.⁵ To circumvent this bottleneck, sustained expression

of MCP-1 at the tumor site may be required to enhance the efficacy of the gene therapy using the *MCP-1* gene.

Systemic or local administration of cytokines has been used to enhance the antitumor immune response induced by many cancer vaccines. However, the systemic administration of cytokines resulted in unwanted side effects. Recently, tumor therapy that uses a membrane-bound form of cytokine was developed to reduce the side effects of cytokine in the systemic circulation. These experiments revealed that the membrane-bound form of cytokine not only reduced the side effects, but enhanced the antitumor effects by prolonging the half-life of cytokines in the tumor microenvironment.⁸

These observations prompted us to design the adenovirus vector driving the expression of membrane-bound form of MCP-1 (mMCP-1) and to evaluate its antitumor effects in a model of HCC. We demonstrated that the delivery of the *mMCP-1* gene markedly augmented HSV-tk/GCV suicide gene therapy, compared with that of the soluble MCP-1 (sMCP-1).

MATERIALS AND METHODS

Recombinant adenovirus vectors

Ad-mMCP-1 (Figure 1a) harboring the human *MCP-1* gene and the membrane-spanning domain of the *CX3CL1* gene driven by the human cytomegalovirus

¹Department of Disease Control and Homeostasis, Graduate School of Medical Science, Kanazawa University, Kanazawa, Japan; ²Division of Cellular and Molecular Pathology, Niigata University Graduate School of Medicine, Niigata, Japan and ³Division of Molecular Bioregulation, Cancer Research Institute, Kanazawa University, Kanazawa, Japan. Correspondence: Dr S Kaneko, Department of Disease Control and Homeostasis, Graduate School of Medical Science, Kanazawa University, 13-1 Takara-machi, Kanazawa 920-8641, Japan.

E-mail: skaneko@m-kanazawa.jp

Received 5 July 2011; revised 5 December 2011; accepted 26 January 2012; published online 9 March 2012

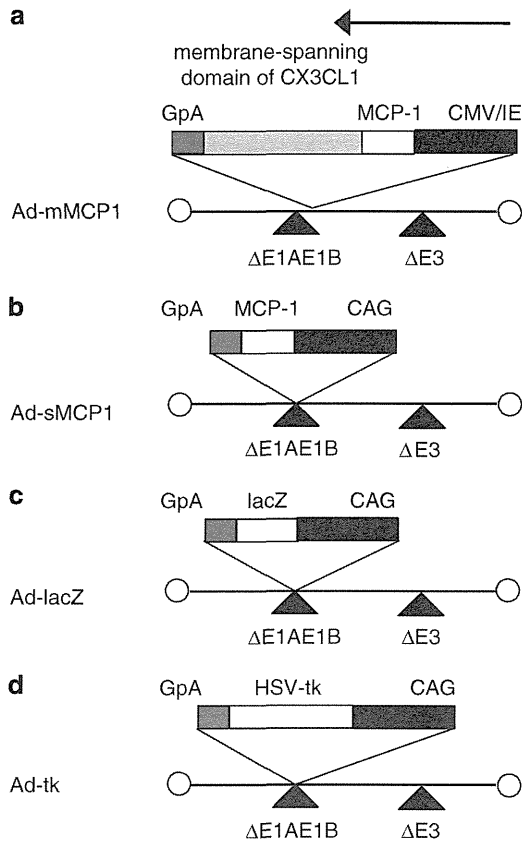


Figure 1. Construct of recombinant adenovirus vector (rAds). Under the control of the cytomegalovirus immediate early promoter/enhancer (CMV/IE) promoter and the CAG promoter, rAd Ad-membrane-bound monocyte chemoattractant protein-1 (mMCP-1) (a) expressing human MCP-1 and the membrane-spanning domain of fractalkine/CX3CL1 in sequence, rAd Ad-soluble-MCP-1 (sMCP-1), (b) expressing MCP-1, rAd Ad-lacZ, (c) expressing lacZ and rAd Ad-tk, (d) expressing HSV-tk. Solid lines indicate the rAd genome. An open triangle below the rAd genome represents a deletion of adenovirus early regions. Arrows show the orientations of the transcription. GpA, rabbit β -globin poly (A) site.

immediate early promoter/enhancer was prepared, purified and titrated according to the protocols supplied by the manufacturer (Takara, Tokyo, Japan). The human MCP-1/CX3CL1 (fractalkine) chimera was designed as follows: DNA encoding a fragment of human CX3CL1 spanning the intracellular, transmembrane and partial extracellular region was amplified from the full-length CX3CL1 cDNA by PCR with the following primers (5'-GCGAGCTCGGGTACCTTCGAGAAGCAGATCG-3' and 5'-GCGAATTCAGATTGTCACACGGGCACAGG-3'). *SacI*, *KpnI* and *EcoRI* restriction enzyme sites were added at the 5' and 3' ends of this fragment. MCP-1 was also amplified by PCR with the following primers (5'-GCGAGCTCGCCAGCATGAAAGTCTCTGCCG-3' and 5'-GCGGTACCAGTCTTCGGAGTTTGGGTTTGC-3'). *SacI* and *KpnI* restriction enzyme sites were added at the 5' and 3' ends of this fragment. The CX3CL1 and MCP-1 DNA fragments were digested with restriction enzymes by coligation into the *SacI* and *EcoRI* sites of pSTBlue-1 (Novagen, Darmstadt, Germany), generating pSTBlue-1-mMCP-1. Then, pSTBlue-1-mMCP-1 was digested by *NotI* and *BamHI* restriction enzymes and the fragment was inserted into the pShuttle Vector (Clontech Laboratories, Mountain View, CA) under the control of cytomegalovirus immediate early promoter/enhancer, generating pShuttle-mMCP-1. The pShuttle-mMCP-1 was digested with *Pi-SceI/I-CeuI* (New England Biolabs, Hitchin, UK) and the purified product was ligated with Adeno-X genome DNA, containing nearly the full length of the adenovirus type 5 genome

lacking the E1 and E3 regions, to generate pAd.mMCP-1. Subsequently, Ad-mMCP-1 was generated by transfecting 293 cells with pAd.mMCP-1, which was linearized with *PacI*, as described in the manual. Ad-sMCP-1 (which expresses sMCP-1), Ad-lacZ (which expresses beta-galactosidase (lacZ)) and Ad-tk (which expresses HSV-tk) were constructed as previously described and propagated in 293 cells (Figures 1b-d).⁹ The rAds were purified on a cesium gradient, and the titer of rAd was determined by the 50% tissue culture infectious dose (TCID₅₀) method.¹⁰

Cell lines and culture

The mouse HCC cell lines (BNL 1NG A2, BNL 1ME A.7R. 1, MM45T.Li and Hepa 1-6) and the colon cancer cell line Colon 26 were used in these experiments. Cells were cultured in Dulbecco's modified Eagle medium (Gibco, Long Island, NY) supplemented with 10% heat-inactivated fetal bovine serum (Gibco).

ELISA for MCP-1

Aliquots of 1×10^5 HCC lines (BNL 1NG A2, BNL 1ME A.7R. 1, MM45T.Li and Hepa 1-6) and the colon cancer cell line, Colon 26 clone 20, were seeded in 1.0 ml of culture media in a six-well tissue culture plate. After 24 h, the cells were infected with Ad-mMCP-1, Ad-sMCP-1 and Ad-lacZ at various multiplicities of infection (MOI). After 48 h, the cells were harvested and sonicated to obtain the membrane fractions, and the media was collected from each well. Tumor tissues were resected on day 1 after subcutaneous injection of 5×10^6 MM45T.Li cells infected with indicated rAds (MOI 50) as described below. Tumor tissues were washed with phosphate-buffered saline (PBS) and sonicated to obtain the membrane fractions. The concentration of MCP-1 was determined by enzyme-linked immunosorbent assay (ELISA) as described previously.¹¹ Briefly, each well of a 96-well microtiter plate was coated with monoclonal anti-human MCP-1 antibody (ME61; 1 mg ml^{-1}) overnight at 41 °C. After washing, the plates were blocked by incubation with PBS containing 1% bovine serum albumin for 1 h at 37 °C. Diluted sample media was added, and the plate was then incubated for 2 h at 37 °C. Following incubation, the plates were washed and incubated with rabbit anti-MCP-1 antibody (1 mg ml^{-1}), followed by alkaline phosphatase-conjugated goat anti-rabbit antibody (1/12 000, Tago, Burlingame, CA), each for 2 h at 37 °C. After the plate was washed, aliquots of 1 mg ml^{-1} p-nitrophenylphosphate (Sigma, St Louis, MO) in 1 M diethanolamine (Sigma; pH 9.8) supplemented with 0.5 mM MgCl₂ were added to the wells, and the plate was incubated for 40 min at room temperature. After the addition of 1 M NaOH, the optical density (405 nm wavelength-OD405) was assessed by using an ELISA plate reader (MTP-120; Corona Electric, Ibaragi, Japan).

In vitro chemotaxis assay

In vitro migration assays were performed with the QCM chemotaxis cell migration assay (5 μm , Chemicon International, Temecula, CA) according to the manufacturer's instructions. Briefly, 7.5×10^4 splenocytes were resuspended in 100 μl of RPMI1640 containing 5% bovine serum albumin, and loaded into the upper well of a transwell chamber. The lower wells were filled with 150 μl of supernatant from MM45T.Li cells that were harvested 48 h after infection with rAds. The cells were incubated for 4 h at 37 °C in a humidified, 5% CO₂ atmosphere. The migrated cells were lysed and detected by the CyQuant GR dye (Molecular Probes, Eugene, OR), and fluorescence was read at an excitation wavelength of 490 nm and an emission wavelength of 520 nm in a fluorescence microplate reader (Thermo Scientific Fluoroskan Ascent FL, Thermo Fisher Scientific Oy, Vantaa, Finland).

In vitro proliferation assay

In vitro proliferation assays were performed with the CellTiter 96 Aqueous Non-Radioactive Cell Proliferation Assay (Promega, Madison, WI) according to the manufacturer's instructions. Briefly, aliquots of 1×10^4 MM45T.Li cells that were harvested 24 h after infection with rAds were seeded in a 96-well tissue culture plate and incubated for 24 h. MTS [3-(4,5-dimethylthiazol-2-yl)-5-(3-carboxymethoxyphenyl)-2-(4-sulphophenyl)-2H-tetrazolium] solution was added and incubated for 2 h, and the absorbance

at 490 nm was measured by using an ELISA plate reader (MTP-120; Corona Electric).

Animal studies

The following investigations were performed in accordance with the guidelines of our Institutional Animal Care and Use Committee. Six-week-old immunocompetent female BALB/c-jcl mice (CLEA Japan, Tokyo, Japan) were injected subcutaneously on both sides of the flank on day 0 with 3×10^5 MM45T.Li cells infected with each rAd at an *in vitro* MOI of 5. For the next 5 days (days 1–5), mice received 75 mg kg^{-1} of intraperitoneally administered GCV (Tanabe Pharmaceutical Drug, Tokyo, Japan). In some series of experiment, $1 \mu\text{g}$ of the recombinant human MCP-1 in $200 \mu\text{l}$ of PBS containing 1% bovine serum albumin were injected intraperitoneally, as previously described,¹² from days 0 to 2 (3 consecutive days) in the group of the tumor cells transduced with Ad-lacZ on HSV-tk/GCV suicide therapy. Tumor sizes were measured every 3 days, and tumor volumes were calculated according to the formula (longest diameter)/(shortest diameter)²/2.

Immunohistochemical analysis

Tumor tissues and spleens were resected on day 10. The tissue samples were embedded in OCT compound (Sakura Finetek, Torrance, CA) and snap-frozen in liquid nitrogen. Cryostat sections of the frozen tissues were fixed with 4% paraformaldehyde in PBS, followed by washing once with distilled water for 5 min and three times with PBS for 5 min. To avoid nonspecific staining, avidin and biotin in the tissues were blocked by using a blocking kit (Vector Laboratories, Burlingame, CA).

The tissue sections were subsequently stained with rat anti-mouse CD4 Ab, rat anti-mouse CD8a Ab, rat anti-mouse CD11b Ab (BD Biosciences, San Diego, CA), or monoclonal mouse anti-human MCP-1 Ab (R&D systems, Minneapolis, MN) overnight at 4°C . Isotype controls were also used. Then, the slides were incubated for 0.5 h at room temperature with biotinylated polyclonal rabbit anti-rat IgG (Dako Cytomation, Tokyo, Japan), or the antibodies in the M.O.M. immunodetection kit to detect mouse primary antibodies on mouse tissues (Vector Laboratories). The reactions were visualized by using a VectaStain ABC standard kit (Vector Laboratories), followed by counterstaining with hematoxylin. The positive cells were counted in 10 randomly chosen fields at 400-fold magnification by an examiner without any prior knowledge of the experimental procedures.

Quantitative real-time reverse-transcriptase PCR

Total RNA was extracted from tumor tissues resected on day 10 using an RNeasy Mini kit (Qiagen, Hilden, Germany) according to the manufacturer's instructions. After treating the RNA preparations with ribonuclease-free DNase I (Qiagen) to remove residual DNA, cDNA was synthesized as described previously.¹³ Quantitative real-time PCR was performed on a StepOne real-time PCR system (Applied Biosystems, Foster City, CA) by using the comparative C_T quantification method. TaqMan Gene Expression Assays (Applied Biosystems) containing specific primers (assay ID: tumor necrosis factor (TNF), Mm00443258_m1; glyceraldehyde-3-phosphate dehydrogenase (GAPDH), Mm99999915_g1), TaqMan MGB probe (FAM dye-labeled), and TaqMan Fast Universal PCR Master Mix were used with 10 ng cDNA to quantify the expression levels of TNF. Reactions were performed for 20 s at 95°C followed by 40 cycles of 1 s at 95°C and 20 s at 60°C . The GAPDH was amplified as an internal control, and the GAPDH C_T values were subtracted from C_T values of the target genes (C_T). The ΔC_T values of tumors after immune gene therapy with both the suicide gene (HSV-tk system) and rAds were compared respectively.

Flow cytometry

MM45T.Li cells transfected with rAds were resuspended in PBS containing 1% bovine serum albumin and 0.1% sodium azide and incubated for 30 min on ice with PE-conjugated rat anti-human MCP-1 (BD Pharmingen, San Diego, CA). The cells were washed, resuspended in PBS and analyzed in a FACScan with CellQuest software (FACSCalibur, BD Biosciences, San Jose, CA).

Depletion of macrophages/monocytes. Clodronate liposome was prepared and systemic depletion of monocytes/macrophages was performed as previously described.^{14,15} Mice were intraperitoneally injected with $200 \mu\text{l}$ of clodronate liposome five times: days -2, 0, 3, 6 and 10 after tumor injection. PBS-clodronate was given in the same manner as a negative control. Depletion of CD11c-negative monocytes in blood was confirmed by flow cytometry after injection of clodronate liposome.

Statistical analysis

Mean and s.d. or s.e. were calculated for the obtained data. The statistical significance of differences between groups was evaluated by the Mann-Whitney *U*-test. $P < 0.05$ was considered statistically significant.

RESULTS

In vitro and *in vivo* MCP-1 production by cells infected with recombinant adenoviruses

When various tumor cells were infected with either Ad-mMCP-1 or Ad-sMCP-1 at an MOI of 10, the cells did not show any signs of cell death (data not shown). Both types of adenoviruses induced the secretion of human MCP-1 into the supernatants to similar levels in all the cell lines that we examined (Figure 2a). On the contrary, MCP-1 contents in the membrane fractions were higher in the cells infected with Ad-mMCP-1 than in those with Ad-sMCP-1 (Figure 2a). The proportion of MCP-1-positive cells were progressively augmented in MM45T.Li cells as the MOIs of the used Ad-mMCP-1 were increased (Figure 2b). In contrast, MCP-1-positive cells were not detected in tumor cells infected with Ad-sMCP-1 and Ad-lacZ, even when the cells were infected with either vector at a MOI of 100 (Figure 2b). Thus, Ad-mMCP-1 infection can *in vitro* drive human MCP-1 expression on the cell surface, as well as its secretion into the culture medium. These results indicate that large amounts of MCP-1 protein were expressed and accumulated on the tumor cell surface when tumor cells were infected with Ad-mMCP-1 as compared with Ad-sMCP-1 *in vitro*. To define the biological functions of secreted human MCP-1 protein, we examined the migratory capacity of splenocytes to the culture supernatants obtained 24 h after the infection. The supernatants from either Ad-mMCP-1- or Ad-sMCP-1-infected cells enhanced the transmigration of splenic lymphocytes to similar extents, compared with those from Ad-lacZ-infected cells (Figure 2c). These results indicated that biologically active human MCP-1 was secreted into the culture supernatants.

Proliferation of tumor cells infected with rAds *in vitro* and *in vivo*

To quantify the proliferation of tumor cells infected with rAds, the MTS assay was performed 24 h after infection. The optical absorbance at 490 nm of tumor cells did not change in the presence or absence of rAd infection (Figure 3a). Next, tumor cells infected with rAds (MOI 10) *ex vivo* were transferred subcutaneously in syngeneic wild-type mice, and tumor development was monitored (Figure 3b). Tumor cells infected with Ad-mMCP-1 and Ad-sMCP-1 showed similar growth rates to tumor cells infected with Ad-lacZ. These results indicate that infection with the rAds used in this study did not affect the proliferation of tumor cells *in vitro* and *in vivo*, and that the delivery of mMCP-1 did not display antitumor activity when used alone. In addition, the levels of MCP-1 expression were confirmed immunohistochemically in the subcutaneous tumor tissues (Figure 3c). MCP-1-positive tumor cells were detected in tumor tissues infected with Ad-mMCP-1; however, the cells were negative for MCP-1 staining in tissues infected with Ad-sMCP-1 and Ad-lacZ. Moreover, larger amounts of MCP-1 were detected in the tumor tissues of the mice treated with Ad-mMCP-1 than in those with Ad-sMCP-1 (Figure 3d). The data indicated that large amounts of MCP-1 protein were expressed and accumulated on the tumor cell surface when the tumor cells were infected with Ad-mMCP-1 *in vivo*.

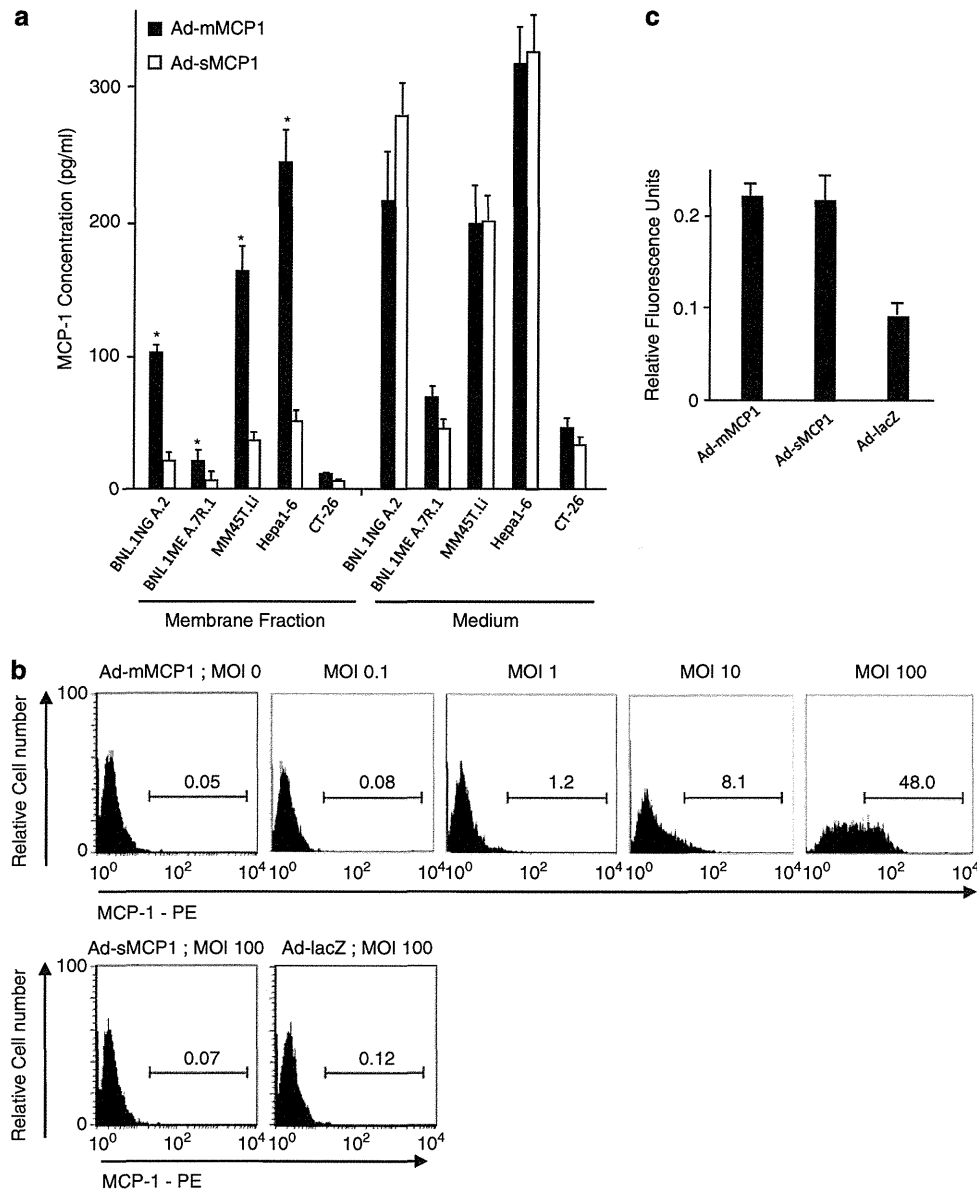


Figure 2. Monocyte chemoattractant protein-1 (MCP-1) production in tumor cells infected with recombinant adenovirus vectors (rAds). **(a)** Concentrations of MCP-1 in the membrane fractions and in the media of hepatoma cells (BNL 1NG A.2, BNL 1ME A.7R.1, MM45T.Li and Hepa1-6) and colon cancer cells (colon 26 clone 20) infected with rAds at multiplicities of infection (MOI) of 10 were measured by enzyme-linked immunosorbent assay (ELISA). Each value is the mean s.d. of triplicate experiments. *, $P < 0.05$ when compared with Ad-soluble MCP-1 (sMCP-1) by the Mann-Whitney's *U*-test. **(b)** Surface expression of MCP-1 on MM45T.Li cells infected with rAds (Ad-mMCP-1, Ad-sMCP-1 and Ad-lacZ) at the indicated MOIs was assessed by flow cytometry by using PE-conjugated anti-human MCP-1 antibody. Histograms represent MCP-1 staining of tumor cells. Numbers indicate percentages of MCP-1-positive cells. Surface MCP-1-positive cells were detected in 0.08, 1.2, 8.1 and 48.0% of MM45T.Li cells infected by Ad-mMCP-1 at MOIs of 0.1, 1, 10 and 100, respectively. The results are representative of three independent experiments. **(c)** The migratory activity of MCP-1 secreted from rAd-infected tumor cells. Mouse splenic lymphocytes were loaded into the upper wells of transwell chambers, and supernatants of tumor cells infected with rAds at an MOI of 10 were added to the lower wells. Cells that migrated through the 8- μ m pores to the feeder tray after 4 h incubation were lysed and detected by CyQuant GR dye that exhibits enhanced fluorescence upon binding cellular nucleic acids. Each value is the mean s.e. of data from three separate migration chambers.

Potential of HSV-tk/GCV suicide therapy by co-infection with Ad-mMCP-1

We previously demonstrated that the gene delivery of Ad-sMCP-1 enhanced the antitumor effects of the HSV-tk/GCV system.^{4-6,16,17} Hence, we compared the effects of Ad-mMCP-1 and Ad-sMCP-1 infection on HSV-tk/GCV suicide therapy. When MM45T.Li cells were co-infected with Ad-tk and Ad-lacZ, and received GCV, tumor growth was delayed marginally but not significantly (Figure 4a).

Co-infection with Ad-tk and Ad-sMCP-1 retarded tumor growth significantly after GCV treatment. Moreover, tumor growth was almost abrogated by the combination of co-infection with Ad-tk and Ad-mMCP-1, and GCV treatment. To address whether the antitumor effects could be induced not only by the gene delivery using Ad vector, but also by the administration of recombinant protein, we gave intraperitoneally recombinant MCP-1 to the animals, which were injected with tumor cells, treated with

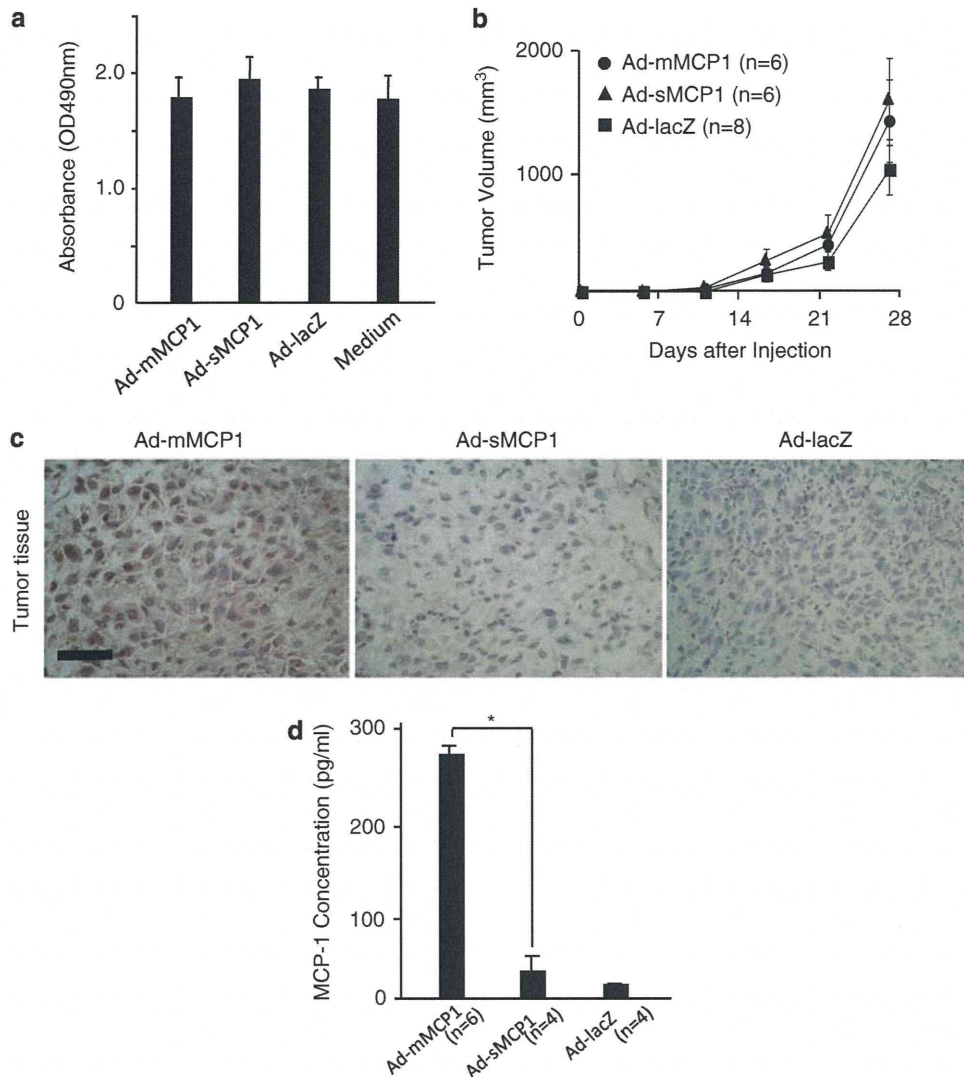


Figure 3. Proliferation of tumor cells infected with recombinant adenovirus vectors (rAds) *in vitro* and *in vivo*. **(a)** Tumor cell growth after the infection of indicated rAds *in vitro*. A total of 5×10^5 of MM45T.Li cells were infected with the rAds at multiplicities of infection (MOI) of 10 and incubated for 24 h. The cell numbers were quantitated by MTS (3-(4,5-dimethylthiazol-2-yl)-5-(3-carboxymethoxyphenyl)-2-(4-sulfophenyl)-2H-tetrazolium) assay. The absorbance was determined at 490 nm with a microplate reader. Each value is the mean s.d. of data from triplicate experiments. **(b)** Tumor cell growth after infection of indicated rAds in mice. BALB/c mice were subcutaneously injected with 3×10^5 MM45T.Li cells infected with the rAds at an MOI of 10 on day 0. Tumor diameters were monitored. Each value is the mean s.e. **(c)** Immunohistochemical analysis of subcutaneous tumor tissues 7 days after the injection in panel **b**. Tissues were stained and visualized by using anti-human monocyte chemoattractant protein-1 (MCP-1) Ab and ABC methods. MCP-1 expression was seen as brown in the cytoplasm of tumor cells. The bar represents 30 μ m. Original magnification, $\times 400$. **(d)** Concentrations of MCP-1 were measured in the s.c. tumor tissues resected on day 1 after injection of 5×10^6 MM45T.Li cells infected with the indicated rAds at an MOI of 50 by enzyme-linked immunosorbent assay (ELISA). Each value is the mean s.d. of duplicate experiments. $*P < 0.05$ when compared with Ad-sMCP-1 by the Mann-Whitney's *U*-test.

Ad-lacZ and Ad-tk. The systemic administration of recombinant MCP-1 rather enhanced tumor growth (Figure 4b). As we previously demonstrated that MCP-1 can promote tumor growth in a context-dependent manner by recruiting macrophages, which can secrete an angiogenic factor, the vascular endothelial growth factor,^{16,18} systemic MCP-1 injection may promote tumor growth by its pro-angiogenic activities.

Recruitment and activation of macrophages and T lymphocytes in tumor tissues

The GCV treatment following co-infection with Ad-lacZ and Ad-tk failed to increase the intratumoral numbers of Mac-1-positive

macrophages, CD4-positive lymphocytes and CD8-positive lymphocytes, compared with GCV treatment following Ad-lacZ infection (Figures 5A and B). GCV administration following co-infection with Ad-sMCP-1 and Ad-tk increased the intratumoral Mac-1-positive macrophage, CD4-positive lymphocyte and CD8-positive lymphocyte numbers (Figure 5A and B). The increases were further enhanced by GCV treatment following co-infection with Ad-mMCP-1 and Ad-tk (Figures 5A and B). Moreover, intratumoral mRNA expression of TNF, a known macrophage and T lymphocyte secretagogue, was markedly enhanced in tumors co-infected with Ad-mMCP-1, compared with those with Ad-sMCP-1 plus Ad-tk. To evaluate the functional contribution of intratumoral immune cells, we depleted CD11c-negative

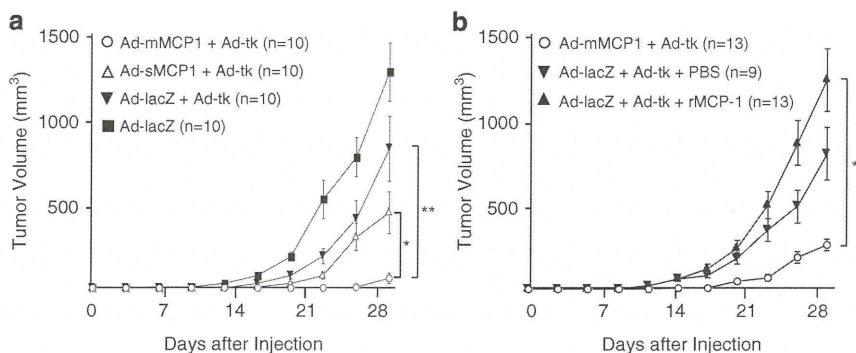


Figure 4. Antitumor effects of recombinant adenovirus vector (rAds) *in vivo*. (a) BALB/c mice were subcutaneously injected with 3×10^5 MM45T.Li cells infected with rAds Ad-membrane-bound monocyte chemoattractant protein-1 (mMCP-1) + Ad-tk, Ad-soluble MCP-1 (sMCP-1) + Ad-tk, Ad-lacZ + Ad-tk, and Ad-lacZ at multiplicities of infection (MOI) of 10 on day 0. Subsequently, 75 mg kg^{-1} of ganciclovir (GCV) was administered for 5 consecutive days (days 2–6). Each value is the mean s.e. of triplicate experiments. $*P < 0.05$ when compared with Ad-sMCP-1 + Ad-tk, and $**P < 0.01$ when compared with Ad-lacZ + Ad-tk by the Mann-Whitney's *U*-test. (b) BALB/c mice were injected with MM45T.Li cells and treated as described in the legend to (a). In Ad-lacZ + Ad-tk + recombinant human MCP-1 (rMCP-1) group, the mice were injected with $1 \mu\text{g}$ of rMCP-1 intraperitoneally from days 0 to 2 (3 consecutive days). The mice were injected with phosphate-buffered saline (PBS) as controls. Tumor sizes were measured every 3 days. Each value is the mean s.e. $**P < 0.01$ when compared with Ad-lacZ + Ad-tk + rMCP-1 by the Mann-Whitney's *U*-test.

monocytes/macrophages by intraperitoneal administration of clodronate liposome in the current mouse model. The monocyte/macrophage-depleted mice developed larger tumor than those treated with PBS liposome (Figure 5D), indicating that monocytes/macrophages were critically involved in the suppression of tumor growth by Ad-mMCP-1. Collectively, these data demonstrate that the delivery of mMCP-1 promoted the recruitment and activation of macrophages and T lymphocytes in tumor tissues, presumably leading to the beneficial antitumor responses in this model.

DISCUSSION

We have proposed a strategy for improving the efficacy of suicide gene-based gene therapy by the combined heterochronic administration of *HSV-tk* and *MCP-1* genes.^{4-6,16-18} In the current study, we generated recombinant adenovirus Ad-mMCP-1 expressing a fusion protein containing the human MCP-1 cDNA fused with the membrane-spanning domain of fractalkine/CX3CL1, to drive more efficient and sessile expression of MCP-1. Ad-mMCP-1 infection did not affect the proliferation of MM45T.Li tumor cells *in vitro* or *in vivo*, by itself. Of interest is that Ad-mMCP-1 infection potentiated HSV-tk/GCV suicide therapy more efficiently than Ad-sMCP-1. Moreover, Ad-mMCP-1-mediated antitumor effects were associated with the recruitment and activation of macrophages and T lymphocytes in tumor tissues. Collectively, the delivery of membrane-bound *MCP-1* gene can augment antitumor effects caused by the HSV-tk/GCV system in an immunocompetent mouse model of liver tumor and therefore, can be a novel strategy of immune-based gene therapy to prevent tumor proliferation and recurrence in patients with HCC.

Chimeric membrane-bound cytokine gene expression vectors were generated to drive the efficient expression on tumor cell surface and to reduce the severe side effects caused by systemic administration of high doses of cytokines. With this maneuver, cytokines can be anchored on the cell plasma membrane. As a consequence, a locally high concentration of cytokines can be achieved with ease and their *in vivo* half-life can be prolonged in the tumor site. The availability of cytokines on tumor cell surface can eventually bring immune cells to the tumor site for better antigen uptake and stimulation, thereby inducing antitumor effects at a higher efficiency. On the basis of these assumptions, this type of modified cytokine gene therapy has been reported on interleukin-2,^{13,19,20} interleukin-12,²¹ fractalkine (CX3CL1)²² and

TNF.²³ Indeed, accumulating evidence revealed that the membrane-bound form of cytokine genes can exhibit more antitumor effects than the corresponding soluble ones. Likewise, the current study confirms that the membrane-bound form of MCP-1 can attract more immune cells, including monocytes/macrophages and T lymphocytes, to the tumor sites and can induce the expression of TNF. In addition, TNF can activate endothelial cells to express several adhesion molecules, such as the intercellular adhesion molecules and vascular cell adhesion molecules.²⁴⁻²⁷ Circulating immune cells can utilize these adhesion molecules to effectively transmigrate into the tissues in addition to the direct chemotactic activities exerted by MCP-1.

The effects of MCP-1 on tumor growth was controversial, either destructive²⁸⁻³⁰ or protective^{31,32} in a context-dependent manner. Likewise, murine colon carcinoma cell expressing MCP-1 failed to metastasize when injected into mice,²⁸ whereas other carcinoma cells showed enhanced metastasis.³¹ These discrepancies may be explained by the observations reported by Nesbit *et al.*³³ They demonstrated that low-level MCP-1 secretion with modest monocyte infiltration resulted in tumor formation, whereas high secretion was associated with massive monocyte/macrophage infiltration into the tumor mass, leading to its destruction within a few days. Thus, systemic MCP-1 administration may not be able to induce massive monocyte/macrophage infiltration into tumor mass and may promote tumor mass as we observed in the present study. Moreover, we previously revealed that suicide therapy can induce tumor cell apoptosis and that apoptotic tumor cells can secrete MCP-1 more efficiently, thereby recruiting a massive number of macrophages and retarding tumor growth.⁴ Consistently, we further demonstrated that the delivery of an optimal amount of rAd expressing MCP-1 enhanced the antitumor effects of the HSV-tk/GCV system in a model of HCC.^{16,18} Infection with Ad-mMCP-1 can sustain MCP-1 expression in tumor tissues more efficiently than that with Ad-sMCP-1 as evidenced by an immunohistochemical analysis on the infected tumor tissues. The sustained MCP-1 expression can potentiate suicide gene therapy more efficiently.

The present data suggest that the use of Ad-mMCP-1 can be promising, but several problems remain to be solved before the clinical application. First, subcutaneous tumor models of an HCC cell line may not be relevant to HCCs in patients. However, in cases of nonsurgical procedures for HCC treatment in patients, such as percutaneous radiofrequency ablation therapy³⁴ and

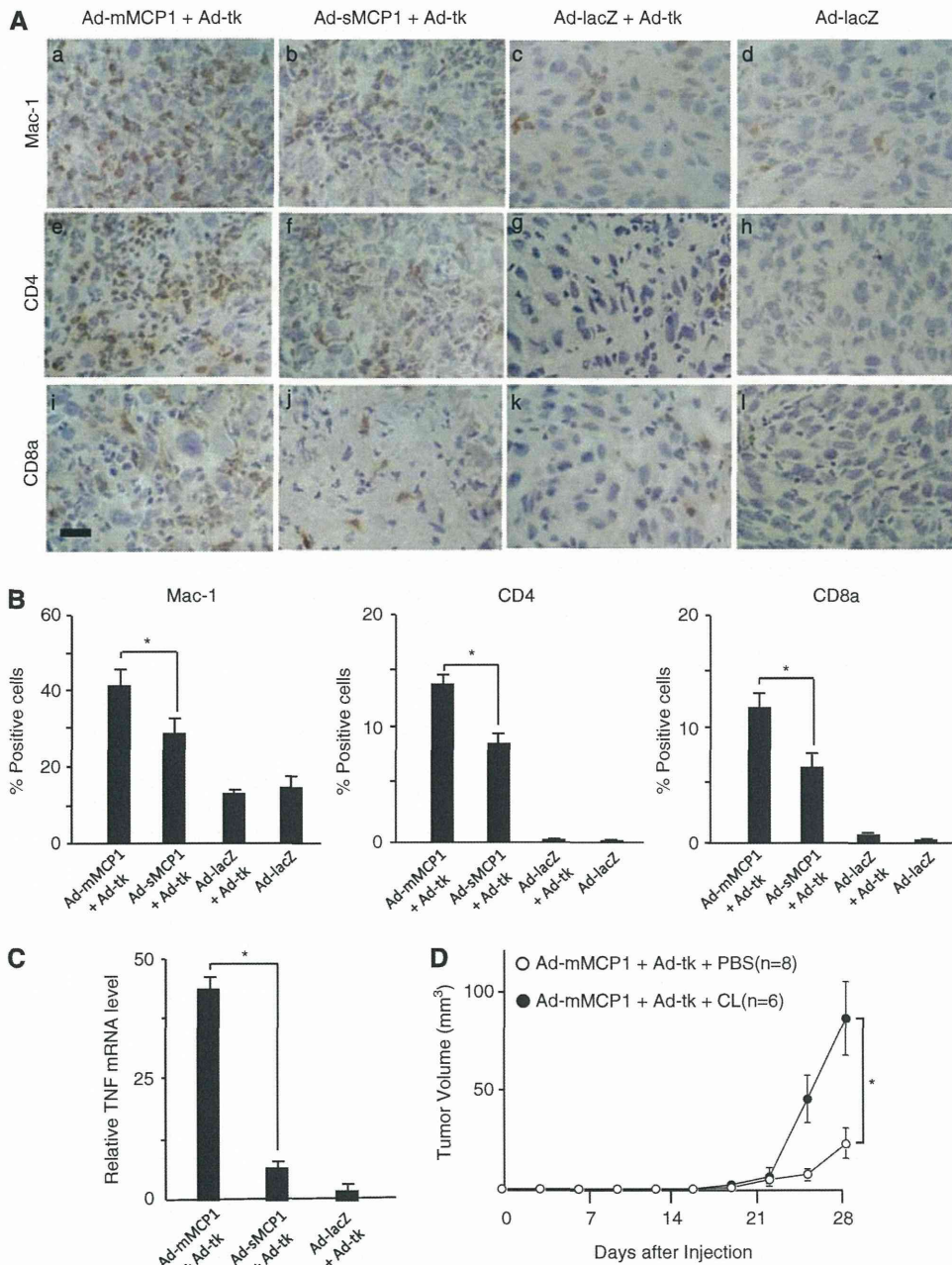


Figure 5. Immunohistochemical analysis for Mac-1-, CD4- and CD8a-positive cells and expression of tumor necrosis factor (TNF) mRNA in tumor tissues. In the experiment described in the legend to Figure 4, tumors were resected on day 10 and used for the analyses. **(A)** Tumor tissues treated with Ad-membrane-bound monocyte chemoattractant protein-1 (mMCP-1) + Ad-tk (a, e and i), Ad-soluble MCP-1 (sMCP-1) + Ad-tk (b, f and j), Ad-lacZ + Ad-tk (c, g and k) and Ad-lacZ (d, h and l) were stained with anti-Mac-1 antibody (a–d), anti-CD4 antibody (e–h) or anti-CD8a antibody (i–l). Positive cells are seen as brown. Original magnification, $\times 400$. **(B)** Quantitative morphometric analysis showing the proportions of positive cells in areas of 100 tumor cells. Ten high-power ($\times 400$) fields of tumor tissue were examined. Results are expressed as means per 1000 hepatoma cells. Values are the means s.d. of triplicate experiments. $*P < 0.05$ when compared with Ad-sMCP-1 by the Mann-Whitney's *U*-test. **(C)** Real-time PCR analysis for TNF mRNA expression in tumor tissues, presented relative to glyceraldehyde 3-phosphate dehydrogenase (GAPDH) mRNA. Each value is the mean s.d. of duplicate experiments. $*P < 0.05$ when compared with Ad-sMCP-1 + Ad-tk by the Mann-Whitney *U*-test. **(D)** BALB/c mice were subcutaneously injected with MM45T.Li cells infected with indicated rAds and treated as described in the legend to Figure 4a. In the Ad-mMCP-1 + Ad-tk + clodronate liposome (CL) group, mice were injected with 200 μ l of CL to deplete monocytes/macrophages as described in Materials and methods. The mice were injected with phosphate-buffered saline (PBS) liposome as controls. Tumor sizes were measured every 3 days. Each value is the mean s.e. $*P < 0.05$ when compared with Ad-mMCP-1 + Ad-tk + PBS by the Mann-Whitney's *U*-test.

transcatheter arterial chemotherapy,³⁵ administration of the current rAd vectors could be easily applied, immediately once the standard nonsurgical procedures to ensure tumor cell killing. Moreover, rAd can elicit its immunogenicity or cytotoxicity when

administered in HCC patients, particularly by the use of intraarterial procedures. Actually, the infection of high doses of rAds causes severe unexpected side effects.³⁶ However, the delivery of membrane-bound form of the MCP-1 gene can cause

a high and effective concentration at the tumor sites even when it is administered at a relatively lower titer, and therefore, can evade severe adverse effects caused frequently by the administration of a high titer of adenovirus vectors.

CONFLICT OF INTEREST

The authors declare no conflict of interest.

ACKNOWLEDGEMENTS

We thank Mariko Katsuda for assistance with histopathological analysis and immunohistochemistry, and Maki Kawamura and Chiharu Minami for providing animal care.

REFERENCES

- Venook AP. Treatment of hepatocellular carcinoma: too many options? *J Clin Oncol* 1994; **12**: 1323-1334.
- Trinchet JC, Beaugrand M. Treatment of hepatocellular carcinoma in patients with cirrhosis. *J Hepatol* 1997; **27**: 756-765.
- Bruix J. Treatment of hepatocellular carcinoma. *Hepatology* 1997; **25**: 259-262.
- Sakai Y, Kaneko S, Nakamoto Y, Kagaya T, Mukaida N, Kobayashi K. Enhanced antitumor effects of herpes simplex virus thymidine kinase/ganciclovir system by codelivering monocyte chemoattractant protein-1 in hepatocellular carcinoma. *Cancer Gene Ther* 2001; **8**: 695-704.
- Tsuchiyama T, Kaneko S, Nakamoto Y, Sakai Y, Honda M, Mukaida N *et al*. Enhanced antitumor effects of a bicistronic adenovirus vector expressing both herpes simplex virus thymidine kinase and monocyte chemoattractant protein-1 against hepatocellular carcinoma. *Cancer Gene Ther* 2003; **10**: 260-269.
- Kagaya T, Nakamoto Y, Sakai Y, Tsuchiyama T, Yagita H, Mukaida N *et al*. Monocyte chemoattractant protein-1 gene delivery enhances antitumor effects of herpes simplex virus thymidine kinase/ganciclovir system in a model of colon cancer. *Cancer Gene Ther* 2006; **13**: 357-366.
- Freund CT, Sutton MA, Dang T, Contant CF, Rowley D, Lerner SP. Adenovirus-mediated combination suicide and cytokine gene therapy for bladder cancer. *Anticancer Res* 2000; **20**: 1359-1365.
- Kim YS. Tumor therapy applying membrane-bound form of cytokines. *Immune Netw* 2009; **9**: 158-168.
- Sato Y, Tanaka K, Lee G, Kanegae Y, Sakai Y, Kaneko S *et al*. Enhanced and specific gene expression via tissue-specific production of Cre recombinase using adenovirus vector. *Biochem Biophys Res Commun* 1998; **244**: 455-462.
- Kanegae Y, Makimura M, Saito I. A simple and efficient method for purification of infectious recombinant adenovirus. *Jpn J Med Sci Biol* 1994; **47**: 157-166.
- Ko Y, Mukaida N, Panyutich A, Voitenok NN, Matsushima K, Kawai T *et al*. A sensitive enzyme-linked immunosorbent assay for human interleukin-8. *J Immunol Methods* 1992; **149**: 227-235.
- Nakano Y, Kasahara T, Mukaida N, Ko YC, Nakano M, Matsushima K. Protection against lethal bacterial infection in mice by monocyte-chemotactic and -activating factor. *Infect Immun* 1994; **62**: 377-383.
- Ji J, Li J, Holmes LM, Burgin KE, Yu X, Wagner TE *et al*. Glycoinositol phospholipid-anchored interleukin 2 but not secreted interleukin 2 inhibits melanoma tumor growth in mice. *Mol Cancer Ther* 2002; **1**: 1019-1024.
- Lu P, Li L, Liu G, van Rooijen N, Mukaida N, Zhang X. Opposite roles of CCR2 and CX3CR1 macrophages in alkali-induced corneal neovascularization. *Cornea* 2009; **28**: 562-569.
- Sadahira Y, Yasuda T, Yoshino T, Manabe T, Takeishi T, Kobayashi Y *et al*. Impaired splenic erythropoiesis in phlebotomized mice injected with CL2MDP-liposome: an experimental model for studying the role of stromal macrophages in erythropoiesis. *J Leukoc Biol* 2000; **68**: 464-470.
- Tsuchiyama T, Nakamoto Y, Sakai Y, Mukaida N, Kaneko S. Optimal amount of monocyte chemoattractant protein-1 enhances antitumor effects of suicide gene therapy against hepatocellular carcinoma by M1 macrophage activation. *Cancer Sci* 2008; **99**: 2075-2082.
- Tsuchiyama T, Nakamoto Y, Sakai Y, Marukawa Y, Kitahara M, Mukaida N *et al*. Prolonged, NK cell-mediated antitumor effects of suicide gene therapy combined with monocyte chemoattractant protein-1 against hepatocellular carcinoma. *J Immunol* 2007; **178**: 574-583.
- Kakinoki K, Nakamoto Y, Kagaya T, Tsuchiyama T, Sakai Y, Nakahama T *et al*. Prevention of intrahepatic metastasis of liver cancer by suicide gene therapy and chemokine ligand 2/monocyte chemoattractant protein-1 delivery in mice. *J Gene Med* 2010; **12**: 1002-1013.
- Chang MR, Lee WH, Choi JW, Park SO, Paik SG, Kim YS. Antitumor immunity induced by tumor cells engineered to express a membrane-bound form of IL-2. *Exp Mol Med* 2005; **37**: 240-249.
- Ji J, Li J, Holmes LM, Burgin KE, Yu X, Wagner TE *et al*. Synergistic anti-tumor effect of glycosylphosphatidylinositol-anchored IL-2 and IL-12. *J Gene Med* 2004; **6**: 777-785.
- Nagarajan S, Selvaraj P. Glycolipid-anchored IL-12 expressed on tumor cell surface induces antitumor immune response. *Cancer Res* 2002; **62**: 2869-2874.
- Tang L, Hu HD, Hu P, Lan YH, Peng ML, Chen M *et al*. Gene therapy with CX3CL1/Fractalkine induces antitumor immunity to regress effectively mouse hepatocellular carcinoma. *Gene Ther* 2007; **14**: 1226-1234.
- Rieger R, Whitacre D, Cantwell MJ, Prussak C, Kipps TJ. Chimeric form of tumor necrosis factor-alpha has enhanced surface expression and antitumor activity. *Cancer Gene Ther* 2009; **16**: 53-64.
- Nooijen PT, Eggermont AM, Verbeek MM, Schalkwijk L, Buurman WA, de Waal RM *et al*. Transient induction of E-selectin expression following TNF alpha-based isolated limb perfusion in melanoma and sarcoma patients is not tumor specific. *J Immunother Emphasis Tumor Immunol* 1996; **19**: 33-44.
- Yang L, Froio RM, Sciuto TE, Dvorak AM, Alon R, Luscinskas FW. ICAM-1 regulates neutrophil adhesion and transcellular migration of TNF-alpha-activated vascular endothelium under flow. *Blood* 2005; **106**: 584-592.
- Vanhee D, Delneste Y, Lassalle P, Gosset P, Joseph M, Tonnel AB. Modulation of endothelial cell adhesion molecule expression in a situation of chronic inflammatory stimulation. *Cell Immunol* 1994; **155**: 446-456.
- VandenBerg E, Reid MD, Edwards JD, Davis HW. The role of the cytoskeleton in cellular adhesion molecule expression in tumor necrosis factor-stimulated endothelial cells. *J Cell Biochem* 2004; **91**: 926-937.
- Huang S, Singh RK, Xie K, Gutman M, Berry KK, Bucana CD *et al*. Expression of the JE/MCP-1 gene suppresses metastatic potential in murine colon carcinoma cells. *Cancer Immunol Immunother* 1994; **39**: 231-238.
- Rollins BJ, Sunday ME. Suppression of tumor formation *in vivo* by expression of the JE gene in malignant cells. *Mol Cell Biol* 1991; **11**: 3125-3131.
- Nokihara H, Yanagawa H, Nishioka Y, Yano S, Mukaida N, Matsushima K *et al*. Natural killer cell-dependent suppression of systemic spread of human lung adenocarcinoma cells by monocyte chemoattractant protein-1 gene transfection in severe combined immunodeficient mice. *Cancer Res* 2000; **60**: 7002-7007.
- Nakashima E, Mukaida N, Kubota Y, Kuno K, Yasumoto K, Ichimura F *et al*. Human MCAF gene transfer enhances the metastatic capacity of a mouse cachectic adenocarcinoma cell line *in vivo*. *Pharm Res* 1995; **12**: 1598-1604.
- Ueno T, Toi M, Saji H, Muta M, Bando H, Kuroi K *et al*. Significance of macrophage chemoattractant protein-1 in macrophage recruitment, angiogenesis, and survival in human breast cancer. *Clin Cancer Res* 2000; **6**: 3282-3289.
- Nesbit M, Schaidt H, Miller TH, Herlyn M. Low-level monocyte chemoattractant protein-1 stimulation of monocytes leads to tumor formation in nontumorigenic melanoma cells. *J Immunol* 2001; **166**: 6483-6490.
- Curley SA. Radiofrequency ablation of malignant liver tumors. *Ann Surg Oncol* 2003; **10**: 338-347.
- Tung-Ping Poon R, Fan ST, Wong J. Risk factors, prevention, and management of postoperative recurrence after resection of hepatocellular carcinoma. *Ann Surg* 2000; **232**: 10-24.
- Marshall E. Gene therapy death prompts review of adenovirus vector. *Science* 1999; **286**: 2244-2245.

Discrete Nature of EpCAM⁺ and CD90⁺ Cancer Stem Cells in Human Hepatocellular Carcinoma

Taro Yamashita,¹ Masao Honda,¹ Yasunari Nakamoto,¹ Masayo Baba,¹ Kouki Nio,¹ Yasumasa Hara,¹ Sha Sha Zeng,¹ Takehiro Hayashi,¹ Mitsumasa Kondo,¹ Hajime Takatori,¹ Tatsuya Yamashita,¹ Eishiro Mizukoshi,¹ Hiroko Ikeda,¹ Yoh Zen,¹ Hiroyuki Takamura,¹ Xin Wei Wang,² and Shuichi Kaneko¹

Recent evidence suggests that hepatocellular carcinoma (HCC) is organized by a subset of cells with stem cell features (cancer stem cells; CSCs). CSCs are considered a pivotal target for the eradication of cancer, and liver CSCs have been identified by the use of various stem cell markers. However, little information is known about the expression patterns and characteristics of marker-positive CSCs, hampering the development of personalized CSC-targeted therapy. Here, we show that CSC markers EpCAM and CD90 are independently expressed in liver cancer. In primary HCC, EpCAM⁺ and CD90⁺ cells resided distinctively, and gene-expression analysis of sorted cells suggested that EpCAM⁺ cells had features of epithelial cells, whereas CD90⁺ cells had those of vascular endothelial cells. Clinicopathological analysis indicated that the presence of EpCAM⁺ cells was associated with poorly differentiated morphology and high serum alpha-fetoprotein (AFP), whereas the presence of CD90⁺ cells was associated with a high incidence of distant organ metastasis. Serial xenotransplantation of EpCAM⁺/CD90⁺ cells from primary HCCs in immune-deficient mice revealed rapid growth of EpCAM⁺ cells in the subcutaneous lesion and a highly metastatic capacity of CD90⁺ cells in the lung. In cell lines, CD90⁺ cells showed abundant expression of c-Kit and *in vitro* chemosensitivity to imatinib mesylate. Furthermore, CD90⁺ cells enhanced the motility of EpCAM⁺ cells when cocultured *in vitro* through the activation of transforming growth factor beta (TGF- β) signaling, whereas imatinib mesylate suppressed *TGFBI* expression in CD90⁺ cells as well as CD90⁺ cell-induced motility of EpCAM⁺ cells. **Conclusion:** Our data suggest the discrete nature and potential interaction of EpCAM⁺ and CD90⁺ CSCs with specific gene-expression patterns and chemosensitivity to molecular targeted therapy. The presence of distinct CSCs may determine the clinical outcome of HCC. (HEPATOLOGY 2012;00:000–000)

The cancer stem cell (CSC) hypothesis, which suggests that a subset of cells bearing stem-cell-like features is indispensable for tumor development, has recently been put forward subsequent to advances in molecular and stem cell biology. Liver cancer, including hepatocellular carcinoma (HCC), is a leading cause of cancer death worldwide.¹ Recent studies have shown the existence of CSCs in liver cancer cell lines and primary HCC specimens using various stem cell markers.^{2–7} Independently, we have identified novel HCC subtypes defined by the hepatic stem/progenitor cell markers,

is a leading cause of cancer death worldwide.¹ Recent studies have shown the existence of CSCs in liver cancer cell lines and primary HCC specimens using various stem cell markers.^{2–7} Independently, we have identified novel HCC subtypes defined by the hepatic stem/progenitor cell markers,

Abbreviations: 5-FU, fluorouracil; Abs, antibodies; AFP, alpha-fetoprotein; CK-19, cytokeratin-19; CSC, cancer stem cell; DNs, dysplastic nodules; EMT, epithelial mesenchymal transition; EpCAM, epithelial cell adhesion molecule; FACS, fluorescent-activated cell sorting; HBV, hepatitis B virus; HCC, hepatocellular carcinoma; HCV, hepatitis C virus; HSCs, hepatic stem cells; IF, immunofluorescence; IHC, immunohistochemistry; IR, immunoreactivity; MDS, multidimensional scaling; NBNC, non-B, non-C hepatitis; NOD/SCID, nonobese diabetic, severe combined immunodeficient; NT, nontumor; OV-1, ovalbumin 1; qPCR, quantitative real-time polymerase chain reaction; SC, subcutaneous; Smad3, Mothers against decapentaplegic homolog 3; TECs, tumor epithelial cells; TGF- β , transforming growth factor beta; TIN, tumor/nontumor; VECs, vascular endothelial cells; VM, vasculogenic mimicry; VEGFR, vascular endothelial growth factor receptor.

From the ¹Liver Center, Kanazawa University Hospital, Kanazawa, Ishikawa, Japan; and ²Laboratory of Human Carcinogenesis, Center for Cancer Research, National Cancer Institute, Bethesda, MD.

Received July 9, 2012; revised October 22, 2012; accepted November 6, 2012.

This study was supported by a Grant-in-Aid from the Ministry of Education, Culture, Sports, Science, and Technology of Japan (23590967), a grant from the Japanese Society of Gastroenterology, a grant from the Ministry of Health, Labor, and Welfare, and a grant from the National Cancer Center Research and Development Fund (23-B-5) of Japan. X.W.W. is supported by the Intramural Research Program of the Center for Cancer Research, U.S. National Cancer Institute.

epithelial cell adhesion molecule (EpCAM) and alpha-fetoprotein (AFP), which correlate with distinct gene-expression signatures and prognosis.^{8,9} EpCAM⁺ HCC cells isolated from primary HCC and cell lines show CSC features, including tumorigenicity, invasiveness, and resistance to fluorouracil (5-FU).¹⁰ Similarly, other groups have shown that CD133⁺, CD90⁺, and CD13⁺ HCC cells are also CSCs, and that EpCAM, CD90, and CD133 are the only markers confirmed to enrich CSCs from primary HCCs thus far.^{3-5,10}

Although EpCAM⁺, CD90⁺, and CD133⁺ cells show CSC features, such as high tumorigenicity, an invasive nature, and resistance to chemo- and radiation therapy, it remains unclear whether these cells represent an identical HCC population and whether they share similar or distinct characteristics. In this study, we used fluorescent-activated cell sorting (FACS), microarray, and immunohistochemistry (IHC) techniques to investigate the expression patterns of the representative liver CSC markers CD133, CD90, and EpCAM in a total of 340 HCC cases and 7 cases of mesenchymal liver tumors. We further explored gene- and protein-expression patterns as well as tumorigenic capacity of sorted cells isolated from 15 primary HCCs and 7 liver cancer cell lines in an attempt to identify the molecular portraits of each cell type.

Materials and Methods

Clinical Specimens. HCC samples were obtained with informed consent from patients who had undergone radical resection at the Liver Center in Kanazawa University Hospital (Kanazawa, Japan), and tissue acquisition procedures were approved by the ethics committee of Kanazawa University. A total of 102 formalin-fixed and paraffin-embedded HCC samples, obtained from 2001 to 2007, were used for IHC analyses. Fifteen fresh HCC samples were obtained between 2008 and 2012 from surgically resected specimens and an autopsy specimen and were used immediately to prepare single-cell suspensions and xenotransplantation (Table 1). Seven hepatic stromal tumors (three cavernous hemangioma, two hemangioendothelioma, and two angiomyolipoma) were formalin fixed and paraffin embedded and used for IHC analyses.

Table 1. Clinicopathological Characteristics of HCC Cases Used for Xenotransplantation

ID	Age/ Sex	Etiology	Tumor Size (cm)	Histological Grade	AFP (ng/mL)	DCP (IU/mL)
P1	77/M	Alcohol	12.0	Moderate	198	322
P2	61/F	NBNC	11.0	Moderate	12	3,291
P3	66/M	NBNC	2.2	Moderate	13	45
P4	65/M	HCV	4.2	Poor	13,700	25,977
P5	52/M	HBV	6.0	Moderate	29,830	1,177
P6	60/M	HCV	2.7	Poor	249	185
P7	79/F	HBV	4.0	Poor	46,410	384
P8	77/F	NBNC	5.5	Moderate	17,590	562
P9	71/M	Alcohol	7.0	Poor	3,814	607
P10	51/M	HBV	2.2	Well	<10	21
P11	71/M	Alcohol	2.1	Well	<10	11
P12	60/M	HBV	10.8	Poor	323	2,359
P13	66/M	HCV	2.8	Moderate	11	29
P14	71/M	HCV	7.2	Moderate	235,700	375,080
P15	75/M	HBV	5.5	Poor	<10	97

Abbreviation: DCP, des-gamma-carboxy prothrombin.

Additional details of experimental procedures are available in the Supporting Information.

Results

EpCAM, CD133, and CD90 Expression in HCC. We first evaluated the frequencies of three representative CSC markers (EpCAM⁺, CD90⁺, and CD133⁺ cells) in 12 fresh primary HCC cases surgically resected by FACS (representative data shown in Fig. 1A). Clinicopathological characteristics of primary HCC cases are shown in Table 1. We noted that frequency of EpCAM⁺, CD90⁺, and CD133⁺ cells varied between individuals. Abundant CD90⁺ (7.0%), but almost no EpCAM⁺ cells (0.06%, comparable to the isotype control) were detected in P2, whereas few CD90⁺ (0.6%), but abundant EpCAM⁺ cells (17.5%) were detected in P4. Very small populations of EpCAM⁺ (0.09%), CD90⁺ (0.04%), and CD133⁺ cells (0.05%) were found in P12, but they were almost nonexistent in P8, except for CD90⁺ cells (0.08%) (Fig. 1A). We further evaluated the expression of EpCAM, CD90, and CD133 in xenografts obtained from surgically resected samples (P13 and P15) and an autopsy sample (P14). As a whole, compared to the isotype control, 7 of 15 HCCs contained definite EpCAM⁺ cells (46.7%), whereas only 3 HCCs

Address reprint requests to: Taro Yamashita, M.D., Ph.D., Department of General Medicine, Kanazawa University Hospital, 13-1 Takara-Machi, Kanazawa, Ishikawa 920-8641, Japan. E-mail: taroy@m-kanazawa.jp; fax: +81-76-234-4250.

Copyright © 2012 by the American Association for the Study of Liver Diseases.

View this article online at wileyonlinelibrary.com.

DOI 10.1002/hep.26168

Potential conflict of interest: Nothing to report.

Additional Supporting Information may be found in the online version of this article.